Recognition of microbial viability via TLR8 drives TFH cell differentiation and vaccine responses

Ugolini, Matteo; Gerhard, Jenny; Burkert, Sanne; Jensen, Kristoffer Jarlov; Georg, Philipp; Ebner, Friederike; Volkers, Sarah M.; Thada, Shruthi; Dietert, Kristina; Bauer, Laura

Total number of authors:
29

Published in:
Nature Immunology

Link to article, DOI:
10.1038/s41590-018-0068-4

Publication date:
2018

Document Version
Peer reviewed version

Recognition of microbial viability via TLR8 promotes T follicular helper cell differentiation and vaccine responses

Matteo Ugolini[1]*, Jenny Gerhard[1]*, Sanne Burkert[3]*, Kristoffer Jarlov Jensen[4,5], Philipp Georg[1], Friederike Ebner[6], Sarah Volkers[1], Shruthi Thada[3,7], Kristina Dietert[8], Laura Bauer[9], Alexander Schäfer[10], Elisa T. Helbig[1], Bastian Opitz[1,2], Florian Kurth[1], Saubashya Sur[3], Nickel Dittrich[3], Sumanlatha Gaddam[7], J. Magarian Blander[11], Christine S. Benn[4,12], Ulrike Blohm[10], Achim D. Gruber[8], Andreas Hutloff[9], Susanne Hartmann[6], Mark V. Boekschoten[13], Michael Müller[13,14], Gregers Jungersen[5], Ralf R. Schumann[3], Norbert Suttorp[1,2] and Leif E. Sander[1,2]

[1]Department of Infectious Diseases and Pulmonary Medicine, Charité – Universitätsmedizin Berlin, corporate member of Freie Universität Berlin, Humboldt-Universität zu Berlin, and Berlin Institute of Health, Berlin, Germany.

[2] German Center for Lung Research (DZL)

[3]Institute of Microbiology and Hygiene, Charité University Hospital, Berlin, Germany.

[4]Research Center for Vitamins and Vaccines, Bandim Health Project, Statens Serum Institut, Copenhagen S, Denmark

[5]Section for Immunology and Vaccinology, National Veterinary Institute, Technical University of Denmark, Kgs Lyngby, Denmark

[6]Department of Veterinary Medicine, Institute of Immunology, Freie Universität Berlin, Berlin, Germany

[7]Bhagwan Mahavir Medical Research Centre, Hyderabad, India

[8]Department of Veterinary Pathology, Freie Universität Berlin, Berlin, Germany

[9]Chronic Immune Reactions, German Rheumatism Research Centre, Berlin, Germany

[10]Institute of Immunology, Friedrich-Loeffler-Institut, Federal Research Institute for Animal Health, Greifswald – Island of Riems, Germany

[11]The Jill Roberts Institute for Research in Inflammatory Bowel Disease, Weill Cornell Medicine, New York, NY

[12]OPEN, Odense Patient data Explorative Network, Odense University Hospital/Department of Clinical Research, University of Southern Denmark, Odense, Denmark

[13]Nutrition, Metabolism and Genomics Group, Division of Human Nutrition, Wageningen University, Wageningen, The Netherlands.

[14]Norwich Medical School, University of East Anglia, Norwich, UK.

*These authors contributed equally to this work

Address correspondence to: Leif Erik Sander, leif-erik.sander@charite.de

Live attenuated vaccines are generally highly efficacious and often superior to inactivated vaccines, yet the underlying mechanisms remain largely unclear. Here we identify innate immune recognition of microbial viability as a potent stimulus for T follicular helper (T_{FH}) cell differentiation and vaccine responses. Antigen presenting cells (APC) distinguish viable from dead bacteria through the detection of bacterial RNA via Toll-like receptor (TLR)-8. Live bacteria, bacterial RNA, or synthetic TLR8 agonists induce a specific cytokine profile in human and porcine APC and promote T_{FH} cell differentiation, which dead bacteria and other TLR ligands fail to induce. Accordingly, vaccination with live, but not heat killed attenuated bacteria induces T_{FH} cell differentiation and robust humoral immune responses in swine. A hypermorphic TLR8 polymorphism was associated with enhanced protective immunity elicited by a live bacterial vaccine against tuberculosis in a human cohort. We provide mechanistic insights into the superiority of live vaccines and we identify TLR8 as a key regulator of T_{FH} cell differentiation and a promising target for T_{FH}-skewing adjuvants.

INTRODUCTION

Live attenuated microbes represent the first generation of vaccines and have contributed to the extinction or dramatic reduction of deadly diseases such as smallpox or rabies[1, 2, 3]. Their unparalleled success was based on empiricism[4]. Yet, their exact mechanisms of action, the frequently observed superiority over inactivated vaccine preparations[5, 6], and their exceptional capacity to induce protective, often lifelong immunity still remain largely unexplained.

As the first line of defense, the innate immune system detects microbial invaders and carefully scales the level of infectious threat in order to elicit appropriate, well-measured immune responses[7]. We have previously described an inherent capacity of murine innate immune cells to discriminate live from dead microorganisms[8]. Viable and thus potentially harmful microorganisms contain specialized pathogen associated molecular patterns (PAMPs) as molecular signatures of microbial life, which we termed *vita*-PAMPs[8]. We identified bacterial messenger RNA as a *vita*-PAMP, detection of which alerts the innate immune system, elicits specific inflammatory immune responses, and promotes humoral immunity in mice[8]. However, the role of *vita*-PAMPs and their receptors in regulating human immune responses is unknown.

Given the importance of innate immune signals in shaping adaptive immune responses[9], we asked whether innate immune recognition of bacterial viability affects ensuing T helper cell responses and particularly the differentiation of T follicular helper (T_{FH}) cells. Since their identification[10, 11], this subset of $CD4^+$ T cells has progressively emerged as a pivotal regulator of the germinal center response and humoral immunity[12, 13, 14]. Differentiation of T_{FH} cells constitutes a complex, multilayered process involving the combination of several molecular and cellular signals at distinct microanatomical sites[12, 13, 14]. Intense research in recent years has unraveled the complexity of T_{FH} cell development, their transcriptional control[14, 15, 16, 17], and their molecular interactions with B cells in the germinal centers, following the initial priming in the T cell zone[18, 19, 20, 21]. Far less is known about the early stages of T_{FH} differentiation and the role of APC-derived innate immune signals in controlling this process, especially in humans. Targeted mobilization of T_{FH} responses poses a major hurdle in vaccine development. Therefore, the identification of particular innate immune pathways with T_{FH}-skewing capacity in humans would be highly desirable for the rational design of T_{FH}-targeted vaccine adjuvants.

In this study, we systematically compared human immune responses to live and dead attenuated bacteria and found that innate immune recognition of bacterial viability leads to transcriptional remodeling in professional APC, and induces T_{FH} promoting signals, most importantly IL-12. Human APC distinguish precisely between viable and dead bacteria independently of virulence, through the detection of bacterial RNA via the endosomal RNA sensor TLR8. Recognition of live bacteria by human APC promotes the differentiation of naïve $CD4^+$ T cells into IL-21 producing $BCL6^+CXCR5^+ICOS^+PD1^+$ T_{FH} cells. Activation of TLR8 in APC by its natural ligand bacterial RNA, or by synthetic agonists promotes subsequent T_{FH} cell differentiation. In contrast, killed bacteria or other TLR agonists, including licensed vaccine adjuvants, which were tested head-to-head with TLR8 agonists, failed to do so even at high concentrations. Consequently, TLR8 gene silencing in APC inhibited bacterial-induced T_{FH} programming. Confirming the importance of viability recognition *in vivo*, we observed robust T_{FH} differentiation in swine in response to immunization with a live attenuated strain of *Salmonella enterica* serovar Typhimurium, a commonly used vaccine in pig farming. This is the first description of T_{FH}-like cells in pigs, which were not increased after immunization with the heat killed version of the same vaccine. Outbred farm pigs represent a valuable immunological model and they are a major target population for prophylactic vaccines, in order to decrease antibiotic consumption and the development of antibiotic resistance. Finally, a case-control study revealed a strong association of a hypermorphic *TLR8* polymorphism and *Bacillus Calmette-Guérin* (BCG)-induced protection from tuberculosis infection, linking TLR8 function to protective immunity in response to a live attenuated vaccine in humans. In summary, we identify recognition of bacterial viability as a conserved innate immune checkpoint that preferentially promotes T_{FH} cell differentiation and humoral immunity. Our study highlights the importance of studying innate immunity in humans and we propose *vita*-PAMP receptors such as TLR8 as promising targets for T_{FH}-skewing adjuvants to improve the efficacy of modern subunit vaccines.

RESULTS

Detection of live bacteria promotes T_{FH} cell differentiation

In order to assess the contribution of innate immune signals on human T_{FH} cell differentiation, we co-cultured classical human $CD14^+CD16^-$ monocytes, as APC, with autologous naïve $CD4^+$ T cells. APC were stimulated with either live avirulent thymidine auxotrophic (*thyA*$^-$, replication defective) *Escherichia coli* (hereafter referred to as EC)[8] or a heat killed versions of the same *E. coli* (HKEC). We intentionally chose avirulent auxotrophic bacteria in order to selectively analyze the impact of bacterial viability without confounding effects due to virulence factors and bacterial replication[8]. Ninety minutes after bacterial stimulation of APC we added antibiotics and naïve CD4 T cells and assessed T helper cell differentiation five days later. Notably, stimulation of APC with live bacteria induced naïve $CD4^+$ T cells to produce large quantities of T_{FH}- and T_H1-signature cytokines IL-21 and interferon-γ (IFN-γ), respectively (**Fig. 1a,b**). This response was virtually absent when APC were stimulated with heat killed bacteria or medium alone (**Fig. 1a,b**). In contrast to IL-21 production, T cell proliferation rates were similar in all conditions, and IL-17 was produced at moderate levels regardless of bacterial viability (**Fig. 1a,b**). In line with the increased IL-21 production, stimulation with viable but not killed bacteria also promoted the expression of prototypical T_{FH} cell surface markers CXCR5, ICOS and PD-1[10, 11, 22] **(Fig. 1c,d** and **Supplementary Fig. 1a)**.

B-cell lymphoma-6 (BCL6) is considered the lineage defining transcription factor of T_{FH} cells, and it is required for successful T_{FH} cell development[16, 17]. APC stimulated with live bacteria induced BCL6 and IL-21 co-expression in $CD4^+$ T cells, whereas APC stimulated with killed bacteria failed to do so (**Fig. 1e,f**). The observed effects were not restricted to monocytes, since similar results were obtained using primary human $CD1c^+$ myeloid dendritic cells (mDC-1) as APC instead of monocytes **(Fig. 1g,h)**. Other T helper cell lineage defining transcription factors T-bet (encoded by *TBX21*) and *GATA-3* were downregulated by bacterial stimulation of APC as compared to T cells activated with unstimulated APC, whereas RORγT (encoded by *RORC*) and *MAF* were slightly increased in both EC and HKEC conditions (**Fig. 1i, Supplementary Fig. 1b**).

Functional properties of de novo *differentiated T_{FH} cells*

Differentiation of T_{FH} cells occurs in a complex multi-step process[12, 13]. An initial priming step involving conventional APC[23] induces transient expression of T_{FH}-associated genes in a subset of

CD4$^+$ T cells[15] allowing for their migration towards the B cell zone within secondary lymphoid organs[12, 24]. There, interaction with B cells, which then take over antigen presentation, stabilizes the T_{FH} differentiation program and initiates the germinal center response[12, 14, 25, 26]. In order to mimic the first two stages of T_{FH} cell differentiation we employed a sequential co-culture system, in which naïve CD4$^+$ T cells were first primed by EC-stimulated monocytes as in Figure 1, re-purified from the culture after five days, and subsequently co-cultured with autologous naïve B cells for an additional seven days. Notably, the T_{FH} phenotype was maintained and increased over the combined culture period of 12 days (**Fig. 2a**) indicating that the initial priming did not merely induce transiently IL-21-expressing effector cells[27].

In order to assess their functionality as *bona fide* B cell helpers, we sorted *de novo* differentiated CD4$^+$CD45RA$^-$CXCR5$^+$ T_{FH} cells and compared them side by side with autologous naïve CD4$^+$CD45RA$^+$CXCR5$^-$ T cells for their ability to promote plasma cell differentiation of co-cultured B cells. Indeed, CXCR5$^+$ T_{FH} generated in response to live bacteria induced robust differentiation of CD27^{++}CD38$^+$ plasma cells, which naïve T cells from the same donor failed to induce (**Fig. 2b,c**). This was also mirrored by the robust IgG production induced by co-culture with *in vitro* differentiated T_{FH} cells, which was not observed with B cells alone or after co-culture with naïve T cells (**Fig. 2d**). CXCR5$^-$ T cells sorted from the same cultures provided relatively weaker help compared to CXCR5$^+$ T cells (**Supplementary Fig. 2a-d**). Collectively, the results demonstrate that innate immune recognition of viable, but not killed bacteria by human APC elicits potent differentiation signals for the generation of fully functional T_{FH} cells.

Detection of bacterial viability uniquely shapes the cytokine profile of APC

In order to characterize the innate immune signals that control T_{FH} programming upon recognition of bacterial viability, we compared the transcriptional responses of human APC to live and dead bacteria. In contrast to the drastically altered T cell responses (**Fig. 1**), detection of live and dead bacteria elicited very similar transcriptional programs in human monocytes (**Fig. 3a**). The highly congruent response to EC and HKEC reflects the high similarity between the two stimuli, both of which contain an abundance of PAMPs and lead to strong APC activation through engagement of a multitude of pattern recognition receptors[8]. Strikingly, a narrow set of 193 genes was differentially regulated in response to live compared to dead bacteria, including the genes encoding for inflammatory cytokines TNF (*TNF*) and IL-12p40 (*IL12B*) (**Fig. 3a,b** and **Supplementary**

Table 1). Accordingly, IL-12 and TNF were released nearly exclusively in response to live but not dead bacteria, whereas other cytokines including IL-6, IL-10, IL-23, and GM-CSF were produced regardless of bacterial viability (**Fig. 3c**). Thus, human APC discriminate precisely between live and dead bacteria and remodel their transcriptional program and subsequent cytokine production in response to the detection of bacterial viability. Differential expression of IL-12 and TNF was unexpected given previous observations in murine APC, which produce large amounts of TNF and IL-12 in response to both live and killed bacteria or purified bacterial cell wall components[8]. Similar to murine APC[8] though, IL-1β release was specifically induced by viable bacteria in human APC indicating inflammasome activation (**Fig. 3c**)[8]. Production of TNF and IL-12 was dependent on the presence of live bacteria and could not be restored by higher doses of killed bacteria (**Fig. 3d**). Other bacterial species, including avirulent Gram-positive *Bacillus subtilis*, and BCG, an attenuated strain of *Mycobacterium bovis* and widely-used live vaccine against tuberculosis (TB), elicited comparable cytokine patterns (**Fig. 3e**), indicating that the response to bacterial viability is conserved and largely independent of bacterial species-specific features. In contrast to the distinct cytokine patterns elicited by live and dead bacteria, both stimuli induced a similar up-regulation of various maturation markers in APC, again emphasizing the intact innate recognition of both stimuli (**Fig. 3f**).

'Viability-induced' T_{FH} responses are mediated by APC-derived IL-12

Based on these results, we hypothesized that APC-derived cytokines were responsible for the observed early T_{FH} differentiation upon detection of live bacteria. Indeed, polyclonally activated $CD4^+$ T cells expressed high levels of IL-21 when differentiated in conditioned culture supernatants from APC that had been stimulated with live bacteria (**Fig. 4a,b**). Conditioned culture supernatants from HKEC-treated APC failed to induce substantial IL-21 production by T cells. Thus, apart from slightly higher background IL-21 and IFN-γ levels, the cell contact-free system essentially reproduced the results of the co-culture experiments, which allow for direct cell contact between APC and T cells (**Fig. 1**). As in the co-cultures, no differences in proliferation rates and IL-17 production were observed (**Supplementary Fig. 3a,b**). These results support a dominant role of APC-derived cytokines in the initial stages of T_{FH} differentiation in response to live EC.

Various cytokines and cytokine combinations have previously been found to promote T_{FH} cell differentiation in mice, including IL-21 itself, IL-6, IL-27 and type I IFN[28, 29, 30, 31], whereas

IL-12, TGF-β, and to a lesser extent IL-23, IL-6, and potentially IL-27, contribute to the differentiation of human T_{FH} cells[30, 32, 33, 34, 35, 36]. Yet it is unclear which cytokines are responsible for infection- or *vita*-PAMP-induced human T_{FH} cell differentiation. We compared cytokine levels in the EC-stimulated APC supernatants with subsequent IL-21 production by $CD4^+$ T cells and found a strong correlation between APC-derived IL-12 levels and subsequent IL-21 production by activated T cells, whereas TNF and IL-6 levels did not correlate with T cell-derived IL-21 (**Fig. 4c**). Neutralization of IL-12 in APC supernatants virtually abolished T_{FH} differentiation, without affecting T cell proliferation rates (**Fig 4d-f** and **Supplementary Fig. 3a**). In contrast, neutralization of IL-6 and IL-27 had no significant effect, whereas TNF blockade partially inhibited T_{FH} differentiation (**Fig. 4d-f**). Conversely, supplementing control-APC supernatants with recombinant IL-12 restored T_{FH} cell differentiation (**Fig. 4d-f**). Recombinant TNF alone was insufficient to promote a T_{FH} phenotype, indicating that it might play a minor role or act in concert with IL-12 or other APC-derived factors (**Fig. 4g**). Recognition of *vita*-PAMPs by APC induces robust production of IL-1β (**Fig. 3c)** and type I IFN[8] in mice. Human T_{FH} cell differentiation was only partially diminished by neutralization of IL-1β and supplementation of control supernatants with recombinant IL-1β alone was insufficient to support T_{FH} cell differentiation (**Supplementary Fig.3d-f**), indicating that IL-1β may have additive effects in humans, consistent with previous observations[32]. Blocking IFN-β or supplementing recombinant IFN-β did not alter human T_{FH} cell differentiation in our experiments (**Supplementary Fig.3d-f**). While additional membrane bound mediators such as ICOSL[20] and OX40L[37] contribute to different stages of T_{FH} differentiation *in vivo*, we found no major differences in the surface levels of both molecules on APC after stimulation with live and dead bacteria (**Fig. 3f**). Although this does not exclude an important role for these membrane-bound molecules at later stages, we conclude that IL-12 is the critical innate immune signal produced in response to live bacteria to instruct early T_{FH} cell priming in humans.

Human APC sense bacterial viability via TLR8

Vaccine adjuvants activate the innate immune system and as such they are essential components of all clinically relevant subunit vaccines[38]. Targeted activation of T_{FH}-polarizing innate immune pathways would be highly desirable for vaccination purposes, given the broad protection offered by high titers of neutralizing and opsonizing antibodies. We therefore investigated the nature of the innate immune receptor(s) and their ligands that elicit 'viability-induced' T_{FH} differentiation

signals in APC. Assuming a critical role for *vita*-PAMPs[8], we supplemented HKEC with various PAMPs and compared subsequent cytokine responses. Only ligands of the endosomal ssRNA receptors TLR7/8 restored IL-12 and TNF production to levels comparable with viable bacteria (**Fig. 5a**). Inhibition of actin polymerization and phagocytosis using Cytochalasin D as well as blockade of endolysosomal acidification with Bafilomycin A abrogated EC-induced production of IL-12 but not IL-6, further suggesting an involvement of endosomal TLRs in the sensing of viable bacteria (**Supplementary Fig. 4a**).

Since human monocytes express TLR8 but only low levels of TLR7 (**Supplementary Fig. 4b**)[39], and TLR8 has been recently shown to recognize bacterial RNA[40, 41], we reasoned that TLR8 might be the primary human *vita*-PAMP receptor for live bacteria. Indeed, endosomal delivery of bacterial RNA fully restored cytokine production to levels comparable to those induced by live bacteria and synthetic TLR7/8 agonists (**Fig 5b**) and induced upregulation of activation markers on APC (**Supplementary Fig. 4c**). Conversely, silencing the expression of TLR8 and its essential signaling adaptor molecule MyD88 by RNA interference abrogated IL-12p70 and TNF release in response to viable EC (**Fig. 5c,d**). Production of IL-6, which does not require bacterial viability, was not affected by TLR8- or MyD88 gene silencing (**Fig. 5c,d**).

These results identify TLR8 as the primary sensor for bacterial viability and critical regulator of cytokine responses, including IL-12 production in human APC.

Detection of bacterial RNA via TLR8 induces T_{FH} differentiation

In line with its critical role in the recognition of live bacteria by human APC, TLR8 ligation dose-dependently induced T_{FH} cell differentiation (**Fig. 6a-c**). In contrast, all other TLR ligands tested, including the licensed vaccine adjuvants monophosphoryl lipid A (TLR4 agonist) and CpG-DNA (TLR9 agonist), failed to promote T_{FH} cell responses even at high concentrations (**Fig. 6a-c**). Similar to live bacteria, TLR8 activation by purified bacterial RNA resulted in high levels of T_{FH} cells and IL-21 production (**Fig. 6d, e**), demonstrating that innate immune recognition of bacterial RNA is a potent stimulator of T_{FH} differentiation signals. Finally, silencing TLR8 expression in APC diminished their capacity to promote T_{FH} differentiation in response to live bacteria (**Fig. 6f, g**). Collectively, these results identify TLR8 as the critical sensor for bacterial viability in human APC and critical inducer of subsequent T_{FH} responses.

Recognition of bacterial viability is conserved in porcine APC

Domestic pigs (*Sus scrofa domestica*) are increasingly utilized for biomedical and pharmaceutical studies due to the substantial analogies between porcine and human physiology[42, 43]. The porcine and the human immune system also shares many similarities[43], including expression and function of TLR8[44]. Owing to the drastic increase in antibiotic resistance rates and frequent emergence of veterinary pathogens in industrial animal farming, there is a growing need for prophylactic vaccines in pigs, making them both an attractive model and a relevant target population for vaccine studies. Here we assessed the relevance of viability recognition for T_{FH} differentiation and vaccine responses in pigs.

Porcine monocytes ($CD172^+CD14^+$) and dendritic cells (DC, $CD172^+CD14^-$) were sorted from spleen samples of domestic pigs and stimulated with live and dead bacteria. We used the thymidine auxotrophic *E. coli* (EC) and an attenuated strain of *Salmonella enterica* serovar Typhimurium (ST) distributed under the trade name of Salmoporc-STM as a live *Salmonella* vaccine for pigs[45]. Salmoporc-STM are histidine- and thymidine auxotrophs leading to severe growth attenuation in the abseence of exogenous histidine and thymidine. Similar to human APC, porcine monocytes and DC secreted high levels of IL-12 in response to live bacteria and TLR8 agonist CL075, but not upon stimulation with heat killed ST (HKST) and HKEC (**Fig. 7a,b)**. Secretion of IL-6 was similarly induced by live and dead bacteria (**Fig. 7a, b**). Selective induction of IL-12 by live bacteria was consinstently observed, yet statistical testing did not reveal significant differences due to high inter-experimental variation in cytokine production. Purified bacterial RNA also promoted increased secretion of IL-12p40 in porcine monocytes, not observed with ligands of TLR2 and TLR4 (**Supplementary Fig. 5**). In order to confirm that the mechanisms of 'viability recognition' are conserved between human and porcine APC, we silenced the expression of TLR8 in porcine $CD14^+$ monocytes by RNAi. Knock down of TLR8 abrogated IL-12p40 expression in response to live ST, whereas IL-6 production, which is induced independently of bacterial viability, was unaffected by TLR8 silencing (**Fig. 7c**). Hence, recognition of bacterial viability requires TLR8 in human and porcine APC. We next assessed the impact of bacterial viability on porcine T_{FH} cell differentiation. Splenocytes (containing APCs and $CD4^+$ T cells) were stimulated with increasing doses of live ST or HKST for one hour, followed by addition of antibiotics to prevent residual bacterial growth. Concanavalin A (ConA) was used to induce polyclonal T cell proliferation. We observed a dose-dependent increase in the frequency of $CD4^+$IL-21^+ $BCL6^+$

T_{FH}-like cells in response to ST, which was absent upon stimulation with HKST, regardless of the bacterial dose (**Fig. 7d,e**). Hence, innate recognition of bacterial viability, i.e. *vita*-PAMPs, specifically controls porcine T_{FH} differentiation. These findings represent the first demonstration of T_{FH}-like cells in swine. When we compared the capacity of soluble PAMPs to induce a T_{FH} phenotype in splenocyte cultures, we found that TLR8 agonists bacterial RNA and CL075, but not TLR4 agonist LPS induced $CD4^+IL21^+$ $BCL6^+$ T cells (**Fig. 7f**). Thus, recognition of bacterial viability via TLR8 plays a critical role for procine T_{FH} cell differentiation.

***Bacterial viability promotes T_{FH} differentiation* in vivo**

To directly assess the role of innate immune detection of bacterial viability for T_{FH} cell responses *in vivo*, we vaccinated domestic pigs with live attenuated ST (Salmoporc-STM), or with an equivalent dose of heat inactivated vaccine (HKST), or solvent as control. Increased frequencies of $CD4^+$IL-21^+ $BCL6^+$ T_{FH}-like cells were detected in the draining (dorsal superficial cervical) lymph node and in the spleen of animals immunized with the live attenuated vaccine compared to animals receiving the heat killed vaccine or saline control (**Fig. 8a, b**). The specific effects of the live vaccine on T_{FH} differentiation was underscored by the fact that other markers of T effector cell differentiation, including lineage defining transcription factors Tbet (T_H1) and FoxP3 (T_{REG}) were similarly altered in T cells from the ST and the HKST vaccine group (**Supplementary Fig 6a-d**).

As a further indication of enhanced follicular helper cell responses following ST vaccination, we observed markedly increased $PAX5^+$ B cell follicles in the spleen of ST vaccinated pigs compared to controls, which was not observed in the HKST group when compared to controls **(Fig. 8c, d**), albeit no statistical difference was detected between the ST and the HKST group. B cell follicles were highly enriched in $KI67^+PAX5^+$ B cells, indicative of active germinal centers (**Fig. 8e, Supplementary Fig. 7a**), but were negative for BCL2 ruling out malignant transformation **(Supplementary Fig. 7b)**. We also found increased $CD3^-CD8^-SLAII^+IgM^+CD2^{+/-}CD21^-$ antibody forming cells (AFC) / plasma cells (PC)[46] in ST- as compared to HKST-vaccinated animals (**Fig. 8f**). Importantly, higher levels of *Salmonella*-binding serum-IgG were detected after vaccination with live ST, as a direct evidence of enhanced humoral immunity in response to the live, compared to the killed vaccine (**Fig. 8g**).

These results corroborated our findings with primary human cells, and they establish the recognition of bacterial viability as an essential driver of vaccine-induced T_{FH} cell responses *in vivo*.

A functional TLR8 polymorphism is associated with vaccine protection in humans

Several functional polymorphisms in the gene encoding for TLR8 in humans have been described[47, 48]. The *TLR8* single nucleotide polymorphism (SNP) TLR8-A1G (rs3764880, hereafter referred to as TLR8-G) alters the start ATG codon into a GTG triplet[47] shifting the signal peptide by three amino acids with a second in frame ATG (M4) being used as alternative start codon. We performed *in silico* modeling predictions, based on the published crystal structure of TLR8[49]. According to these models, the amino acid truncation leads to significant structural alterations of the protein (**Supplementary Figure 8-10 and Supplementary Text**). Increased disorder, free energy, and increased flexibility of TLR8-G likely make the receptor better adapted to side chain rearrangement and dimerization. The larger volume of clefts and cavities on the surface of TLR8-G, compared to TLR8-A, may increase its potential for ligand binding, whereas functional pockets and nests are slightly decreased (**Supplementary Fig. 9, 10**). These models suggest an altered receptor functionality, which may cause a gain-of-function in the TLR8-G variant. In line with these predictions, APC from individuals carrying either the TLR8-A or TLR8-G variant showed a slightly enhanced IL-12 response to TLR8 stimulation, but not in response to TLR4 agonist LPS (**Supplementary Fig. 11a, b**). High inter-donor variation combined with the moderate gain of function phenotype account for the modest, but significant impact on cytokine production. Analysis of TLR8-G and TLR8-A function in a standardized reporter cell system confirmed the gain-of-function phenotype, since reporter cells expressing the TLR8-G variant showed stronger NF-κB activation in response to TLR8 ligands compared to TLR8-A expressing cells (**Supplementary Fig. 11c)**.

Previous studies have associated TLR8-G allele carriage with slower progression of HIV-infection[47], and protection against pulmonary TB (PTB)[50]. Here, we assessed TLR8-G allele distribution in 293 patients with confirmed TB and 165 of their healthy household contacts (**Supplementary Table 2**). Significantly more controls (53.9%) were homo- or hemizygous TLR8-G carriers than TB patients (41.3%) (**Fig. 9a, left panel** and **Supplementary Table 3**). The TLR8-A allele was associated with significantly increased odds for TB infection (OR=1.94 [1.194-

3.156];p=0.007), and similar results were found in the PTB subgroup (**Fig. 9a, right panel** and **Supplementary Table 3**), confirming the protective effect of the TLR8-G allele against PTB as previously reported[50]. However, further subgroup analyses revealed that TLR8 allele distribution was in fact significantly different only in subjects who had previously received the BCG vaccine against TB (p=0.002), whereas allele distribution was not different (p=0.754) in unvaccinated subjects (**Fig. 9b** and **Supplementary Table 4**). Consequently, in this study population, BCG-vaccination is associated with a significant risk protection in TLR8-G carriers (OR=0.280 [CI95% 0.105-0.742]), but not in TLR8-A allele carriers (**Fig. 9c** and **Supplementary Table 4**). These epidemiological results indicate that TLR8-G carriage is associated with an improved BCG-vaccine mediated protection without affecting susceptibility to PTB *per se.* The study links TLR8 function to protective immunity in response to a live bacterial vaccine in a large human cohort.

DISCUSSION

Our study identifies innate immune recognition of microbial viability as a hard-wired, conserved immune checkpoint, which critically regulates innate and adaptive immunity. We describe TLR8 as the first *vita*-PAMP receptor in humans and pigs, activation of which renders APC highly effective inducers of T_{FH} responses. We provide experimental and epidemiological evidence to support a critical function of viability recognition and TLR8 in the immune responses to live attenuated vaccines in humans and pigs.

Recent studies in non-human primates have revealed a unique adjuvant activity of TLR8 agonists[51, 52, 53]. Innate immune responses to TLR8 agonist-containing nanoparticles were highly similar to responses evoked by live BCG, but distinct from those elicited by various inanimate vaccines[51]. Supplementation of the commercial alum-adjuvanted pneumococcal glycoconjugate vaccine (PCV13) with an TLR8 agonist strongly increased IgG responses in newborn rhesus macaques[52]. We show that live attenuated bacteria as well as purified bacterial RNA or synthetic TLR8 agonists selectively modulate the cytokine profile of APC and promote T_{FH} responses, which dead bacteria and other TLR ligands fail to induce. Moreover, we found a functional TLR8 polymorphism to be associated with increased cytokine production in response to TLR8 synthetic ligands and with enhanced protection afforded by BCG vaccination in early life, clearly supporting a link between TLR8 functionality and vaccine responses in humans (**Fig. 9**). These findings may

also help to explain the diverging efficacies of BCG-vaccination reported in various studies[54]. While the role of T_{FH} cells cannot be assessed in this retrospective case-control study, mounting evidence suggest a critical contribution of T_{FH} and a T cell-dependent antibody responses in BCG vaccination and anti-mycobacterial immunity[55, 56, 57, 58]. In particular, IL-12 has been recently linked to the devolpment of T_{FH}-like cells at the site of TB infection[58]. Supporting the notion that BCG vaccination elicits T_{FH} cell dependent responses, we found increased T_{FH} cell frequencies in the spleens of pigs 30 days after BCG vaccination (**Supplementary Fig. 12**). Although commonly used live vaccines are diverse and likely activate multiple pathways[59], we propose innate immune recognition of microbial viability and subsequent promotion of T cell-driven immunity as a unifying motif in the responses to live attenuated vaccines.

In order to further validate our findings, we studied vaccine responses to live attenuated bacteria in pigs. Vaccine studies in large animals such as pigs are challenging, due to obvious limitations in group size and a relative lack of advanced tools and experimental models (e.g. TCR-transgenic or PRR-deficient animals) compared to mice. On the other hand, domestic pigs offer major advantages over established rodent models, given their closer resemblance of human physiology with regards to size, life span, organ anatomy, diet, circadian rhythm, and immunity [42, 60]. Conventional non-specific-pathogen-free(SPF) housing and outbreeding of the animals also makes for a better comparability to humans. More importantly, besides serving as a model, domestic farm animals represent a critical target population for vaccination in order to improve animal- and public health. High antibiotic consumption in industrial animal farming is considered a major driving force of antibiotic resistance[61], and efficacious veterinary vaccines are therefore urgently needed[62]. Here we used a well-established swine vaccine against *Salmonella enterica* infections to dissect the immune responses to live attenuated bacteria in pigs. Our study provides the first evidence of T_{FH}-like cells in pigs and describes their induction upon recognition of bacterial viability *in vitro* and *in vivo* (**Fig. 7 and 8**). While future studies are clearly needed to fully characterize the generation of protective immunity in pigs, our study contributes new insights into the mechanisms of actions of live attenuated vaccines and highlights swine as a valuable species for vaccine and T_{FH} cell research.

In contrast to the detailed knowledge of the transcriptional regulation of T_{FH} cells and their interaction with B cells, few studies have investigated the T_{FH}-polarizing potential of different innate immune stimuli like vaccine adjuvants. The requirement for conventional APC in priming

T_{FH} cell responses is evident[12, 14, 23] and it was previously suggested that innate activation signals could determine the capacity of APC to prime T_{FH} cell responses. Yet, the nature of T_{FH}-favoring innate immune stimuli has remained largely unknown. Several studies have addressed the impact of TLR activation on the development of T_{FH} cells and germinal center formation in mice[63, 64, 65, 66, 67, 68, 69]. For instance, it has been reported that monocyte-derived dendritic cells (Mo-DC) are important stimulators of T_{FH} cell responses in mice, especially when activated via TLR9[70]. However, T_{FH} cell differentiation in mice and humans differs substantially, with regards to the involved cytokines, as well as the innate immune receptor repertoires in mice and human APC. This is exemplified by the differential functionality of human and murine TLR8, the latter being irresponsive to ssRNA[71]. These factors severely hamper the translation of findings from studies in laboratory mice to human T_{FH} cell- and vaccine responses[71]. Human monocytes hardly induce T_{FH} differentiation in response to CpG DNA compared to stimulation with viable bacteria and TLR8 agonists (**Fig. 6a-c**). Previous work suggested that heat killed bacteria and bacterial lipopolysaccharide (LPS) were sufficient to induce T_{FH} cell differentiation by human *in vitro* differentiated Mo-DC[35]. However, Mo-DC produce large quantities of bioactive IL-12, due to the enhancing effects of IL-4 contained in the differentiation medium[72]. In contrast, primary $CD14^+CD16^-$ monocytes, as well as porcine monocytes and DC, secrete high amounts of IL-12 in response to live bacteria and TLR8 ligation, while production of IL-12 and the T_{FH}-skewing capacity is not observed when APC are stimulated with heat killed bacteria or LPS (**Fig. 3, Fig. 6a, b, Fig. 7a and Supplementary Fig. 5**). Moreover, we detected an increase in $CD4^+$IL-21^+ $BCL6^+$ T cells following *ex vivo* culture of porcine splenocytes with increasing doses of ST, which was not observed with HKST (**Fig. 7d-e**). Similarly, $CD4^+$IL-21^+ $BCL6^+$ T cells increased in the draining lymph nodes and in the spleens of pigs following vaccination with a live attenuated *Salmonella* strain, which was not observed upon immunization with the killed version of the same bacterium (**Fig. 8a, b**). The latter contains large quantities of PAMPs, including LPS, yet it did not induce T_{FH} cell differentiation, further underscoring the dependency of T_{FH} cell responses on bacterial viability and *vita*-PAMPs.

So far, primary immunodeficiencies (PID) associated with TLR8 deficiency have not been reported. However, patients with gene defects in TLR adaptor proteins MyD88 or IRAK-4 suffer from PID and show a higher susceptibility to bacterial infection[73, 74]. The frequency of T_{FH} cells has not been investigated in individuals with these rare gene defects.

Individuals harbouring loss of function mutations in the IL-12 receptor (IL12R1B), the cytokine driving T_{FH} cell differentiation in response to TLR8 ligation, display lower numbers of circulating T_{FH} cells and reduced GC formation in lymph nodes[34]. Other studies have reported a less pronounced phenotype in older adults, however these studies investigated fewer individuals[75, 76]. Naïve $CD4^+$ T cells isolated from *IL12R1B* deficient individuals fail to induce IL-21 in respose to IL-12 stimulation *in vitro*[75]. A similar phenotype was observed with T cells from indivudals harbouring a heterozygous *STAT3* deficiency[75], which also exhibit reduced circulating T_{FH} cells[75, 76]. Notably, antibody levels are largely normal in *IL12RB1*-deficient individuals, yet serum IgG against tetanus toxoid have a lower avidity, which was not observed with viral antigens, possibly due to longer persistence of the antigen[34]. These observations highlight our need to better characterize human immune responses in PID patients, which will allow the identification of non-redundant signaling modules, as well as potential compensation mechanisms.

Given the broad functionality of high affinity antibody responses, it has been proposed that any microbial stimulus or PAMP is likely to induce T_{FH} differentiation[12]. Here we challenge this wide-spread notion showing that only viable bacteria and agonists of TLR8 promote robust T_{FH} cell formation (**Fig. 6, 7, 8**) and thus provide insights into the proximal innate sensing events that govern early T_{FH} differentiation.

High affinity antibodies are indeed a versatile mechanism of defense against many pathogens, yet uncontrolled T_{FH} activation can cause autoimmunity and debilitating diseases[22, 77]. We have previously proposed that antimicrobial immune responses are tightly scaled to the level of the microbial threat and we suggested a series of innate immune checkpoints that facilitate an accurate immunological risk assessment[7]. Here we show that the recognition of bacterial RNA, as a molecular signature of microbial viability (*vita*-PAMP)[8], constitutes a critical trigger of T_{FH} differentiation. We propose that the nature and the composition of microbial stimuli, i.e. the presence of *vita*-PAMPs (together with immunogenic antigens), is critical to instruct T_{FH} cell responses. This provides an efficient checkpoint without limiting the versatility of T_{FH} cells in the defense against microbial threats.

The identification of TLR8 as a critical sensor of *vita*-PAMPs and regulator of preferential T_{FH} differentiation provides opportunities for the development of T_{FH}-targeted vaccine adjuvants,

462 which are sorely needed to improve existing and future inanimate subunit vaccines against a broad
463 range of infectious and non-infectious diseases.
464

Acknowledgments:

We thank Désirée Kunkel, Sarah Warth and and Angela Linke for excellent technical assistance. We are indebted to the flow cytometry facility of the Berlin Brandenburg Center for Regenerative Therapies (BCRT) of the Charité Berlin. We thank Dr. Sven Springer and IDT Biologika GmbH, for assistance in designing the animal studies and for kindly providing the Salmoporc STM vaccine. We are thankful to Dr. Riccardo Nifosí of NEST CNR-NANO, Pisa, Italy for his critical review of the modelling analysis of TLR8.

This study was supported by the German Research Council (DFG grant SA1940-2/1 and SFB-TR84 TP C8 to L.E.S., SFB-TR84 TP B1 to N.S., SFB-TR-84 TP A1/A5 to B.O., SFB-TR84 TP Z1b to A.D.G. and the DFG-GRK 1673 project to R.R.S.), the European Research Council and the German Ministry of Science and Education (FP-7 ERA-NET / Infect-ERA consortium "HaploINFECT" to L.E.S.), the European Society of Clinical Microbiology and Infectious Diseases (ESCMID research grant to L.E.S.), the Jürgen Manchot Foundation (Doctoral Research Fellowship to P.G., E.T.H. and S.V.), the Netherlands Nutrigenomics Center, Wageningen University, The Netherlands (to M.M. and M.B.), the National Institute of Diabetes and Digestive and Kidney Diseases (DK072201 to J.M.B.), the National Institute of Allergy and Infectious Diseases (AI073899, AI7570293, AI095245 to J.M.B.), the Fritz Thyssen Foundation (research grant to A.H.), The Danish National Research Foundation (grant no. DNRF108) to Research Centre for Vitamins and Vaccines (CVIVA) supporting K.J.J., and The Novo Nordisk Foundation supporting the pig vaccination experiments at Technical University of Denmark, Federal Ministry of Education and Research (VIP+ VALNEMCYS project to S.H.).

The gene array data will be made publicly available in the public Gene Expression Omnibus database (GEO, GSE68255).

References

1. Barquet, N. & Domingo, P. Smallpox: the triumph over the most terrible of the ministers of death. *Ann Intern Med* **127**, 635-642 (1997).

2. Plotkin, S.A. & Plotkin, S.L. The development of vaccines: how the past led to the future. *Nat Rev Microbiol* **9**, 889-893 (2011).

3. Minor, P.D. Live attenuated vaccines: Historical successes and current challenges. *Virology* **479-480**, 379-392 (2015).

4. De Gregorio, E. & Rappuoli, R. From empiricism to rational design: a personal perspective of the evolution of vaccine development. *Nat Rev Immunol* **14**, 505-514 (2014).

5. Sridhar, S., Brokstad, K.A. & Cox, R.J. Influenza Vaccination Strategies: Comparing Inactivated and Live Attenuated Influenza Vaccines. *Vaccines (Basel)* **3**, 373-389 (2015).

6. Rauh, L.W. & Schmidt, R. Measles Immunization with Killed Virus Vaccine. Serum Antibody Titers and Experience with Exposure to Measles Epidemic. *Am J Dis Child* **109**, 232-237 (1965).

7. Blander, J.M. & Sander, L.E. Beyond pattern recognition: five immune checkpoints for scaling the microbial threat. *Nature Reviews Immunology* **12**, 215-225 (2012).

8. Sander, L.E. *et al.* Detection of prokaryotic mRNA signifies microbial viability and promotes immunity. *Nature* **474**, 385-389 (2011).

9. Iwasaki, A. & Medzhitov, R. Control of adaptive immunity by the innate immune system. *Nat Immunol* **16**, 343-353 (2015).

10. Breitfeld, D. *et al.* Follicular B helper T cells express CXC chemokine receptor 5, localize to B cell follicles, and support immunoglobulin production. *J Exp Med* **192**, 1545-1552 (2000).

11. Schaerli, P. *et al.* CXC chemokine receptor 5 expression defines follicular homing T cells with B cell helper function. *J Exp Med* **192**, 1553-1562 (2000).

12. Crotty, S. T follicular helper cell differentiation, function, and roles in disease. *Immunity* **41**, 529-542 (2014).

13. Ma, C.S., Deenick, E.K., Batten, M. & Tangye, S.G. The origins, function, and regulation of T follicular helper cells. *J Exp Med* **209**, 1241-1253 (2012).

14. Vinuesa, C.G., Linterman, M.A., Yu, D. & MacLennan, I.C. Follicular Helper T Cells. *Annu Rev Immunol* **34**, 335-368 (2016).

15. Hatzi, K. *et al.* BCL6 orchestrates Tfh cell differentiation via multiple distinct mechanisms. *J Exp Med* **212**, 539-553 (2015).

16. Johnston, R.J. *et al.* Bcl6 and Blimp-1 are reciprocal and antagonistic regulators of T follicular helper cell differentiation. *Science* **325**, 1006-1010 (2009).

17. Nurieva, R.I. *et al.* Bcl6 mediates the development of T follicular helper cells. *Science* **325**, 1001-1005 (2009).

18. Cannons, J.L. *et al.* Optimal germinal center responses require a multistage T cell:B cell adhesion process involving integrins, SLAM-associated protein, and CD84. *Immunity* **32**, 253-265 (2010).

19. Linterman, M.A. *et al.* IL-21 acts directly on B cells to regulate Bcl-6 expression and germinal center responses. *J Exp Med* **207**, 353-363 (2010).

20. Weber, J.P. *et al.* ICOS maintains the T follicular helper cell phenotype by down-regulating Kruppel-like factor 2. *J Exp Med* **212**, 217-233 (2015).

21. Good-Jacobson, K.L. *et al.* PD-1 regulates germinal center B cell survival and the formation and affinity of long-lived plasma cells. *Nat Immunol* **11**, 535-542 (2010).

22. Ueno, H., Banchereau, J. & Vinuesa, C.G. Pathophysiology of T follicular helper cells in humans and mice. *Nat Immunol* **16**, 142-152 (2015).

23. Goenka, R. *et al.* Cutting edge: dendritic cell-restricted antigen presentation initiates the follicular helper T cell program but cannot complete ultimate effector differentiation. *J Immunol* **187**, 1091-1095 (2011).

24. Moser, B., Schaerli, P. & Loetscher, P. CXCR5(+) T cells: follicular homing takes center stage in T-helper-cell responses. *Trends Immunol* **23**, 250-254 (2002).

25. Ebert, L.M., Horn, M.P., Lang, A.B. & Moser, B. B cells alter the phenotype and function of follicular-homing CXCR5+ T cells. *Eur J Immunol* **34**, 3562-3571 (2004).

26. Kerfoot, S.M. *et al.* Germinal center B cell and T follicular helper cell development initiates in the interfollicular zone. *Immunity* **34**, 947-960 (2011).

27. Nakayamada, S. *et al.* Early Th1 cell differentiation is marked by a Tfh cell-like transition. *Immunity* **35**, 919-931 (2011).

28. Vogelzang, A. *et al.* A fundamental role for interleukin-21 in the generation of T follicular helper cells. *Immunity* **29**, 127-137 (2008).

29. Eddahri, F. *et al.* Interleukin-6/STAT3 signaling regulates the ability of naive T cells to acquire B-cell help capacities. *Blood* **113**, 2426-2433 (2009).

30. Batten, M. *et al.* IL-27 supports germinal center function by enhancing IL-21 production and the function of T follicular helper cells. *J Exp Med* **207**, 2895-2906 (2010).

31. Cucak, H., Yrlid, U., Reizis, B., Kalinke, U. & Johansson-Lindbom, B. Type I interferon signaling in dendritic cells stimulates the development of lymph-node-resident T follicular helper cells. *Immunity* **31**, 491-501 (2009).

32. Schmitt, N. *et al.* The cytokine TGF-beta co-opts signaling via STAT3-STAT4 to promote the differentiation of human TFH cells. *Nat Immunol* **15**, 856-865 (2014).

33. Ma, C.S. *et al.* Early commitment of naive human CD4(+) T cells to the T follicular helper (T(FH)) cell lineage is induced by IL-12. *Immunol Cell Biol* **87**, 590-600 (2009).

34. Schmitt, N. *et al.* IL-12 receptor beta1 deficiency alters in vivo T follicular helper cell response in humans. *Blood* **121**, 3375-3385 (2013).

35. Schmitt, N. *et al.* Human dendritic cells induce the differentiation of interleukin-21-producing T follicular helper-like cells through interleukin-12. *Immunity* **31**, 158-169 (2009).

36. Diehl, S.A., Schmidlin, H., Nagasawa, M., Blom, B. & Spits, H. IL-6 triggers IL-21 production by human CD4+ T cells to drive STAT3-dependent plasma cell differentiation in B cells. *Immunol Cell Biol* **90**, 802-811 (2012).

37. Jacquemin, C. *et al.* OX40 Ligand Contributes to Human Lupus Pathogenesis by Promoting T Follicular Helper Response. *Immunity* **42**, 1159-1170 (2015).

38. Coffman, R.L., Sher, A. & Seder, R.A. Vaccine adjuvants: putting innate immunity to work. *Immunity* **33**, 492-503 (2010).

39. Hornung, V. *et al.* Quantitative expression of toll-like receptor 1-10 mRNA in cellular subsets of human peripheral blood mononuclear cells and sensitivity to CpG oligodeoxynucleotides. *J Immunol* **168**, 4531-4537 (2002).

40. Eigenbrod, T., Pelka, K., Latz, E., Kreikemeyer, B. & Dalpke, A.H. TLR8 Senses Bacterial RNA in Human Monocytes and Plays a Nonredundant Role for Recognition of Streptococcus pyogenes. *J Immunol* **195**, 1092-1099 (2015).

41. Bergstrom, B. *et al.* TLR8 Senses Staphylococcus aureus RNA in Human Primary Monocytes and Macrophages and Induces IFN-beta Production via a TAK1-IKKbeta-IRF5 Signaling Pathway. *J Immunol* **195**, 1100-1111 (2015).

42. Meurens, F., Summerfield, A., Nauwynck, H., Saif, L. & Gerdts, V. The pig: a model for human infectious diseases. *Trends Microbiol* **20**, 50-57 (2012).

43. Mair, K.H. *et al.* The porcine innate immune system: an update. *Dev Comp Immunol* **45**, 321-343 (2014).

44. Zhu, J., Lai, K., Brownile, R., Babiuk, L.A. & Mutwiri, G.K. Porcine TLR8 and TLR7 are both activated by a selective TLR7 ligand, imiquimod. *Mol Immunol* **45**, 3238-3243 (2008).

45. Lindner, T., Springer, S., Selbitz, H.J. . The use of a Salmonella Typhimurium live vaccine to control Salmonella Typhimurium in fattening pigs in field and effects on serological surveillance. *Proceedings of the 7th International Safepork Symposium on Epidemiology and Control of Foodborne Pathogens in Pork, Verona, Italy*, 237 - 239 (2007).

46. Sinkora, M., Stepanova, K. & Sinkorova, J. Different anti-CD21 antibodies can be used to discriminate developmentally and functionally different subsets of B lymphocytes in circulation of pigs. *Dev Comp Immunol* **39**, 409-418 (2013).

47. Oh, D.Y. *et al.* A functional toll-like receptor 8 variant is associated with HIV disease restriction. *J Infect Dis* **198**, 701-709 (2008).

48. Wang, C.H. *et al.* TLR7 and TLR8 gene variations and susceptibility to hepatitis C virus infection. *PLoS One* **6**, e26235 (2011).

49. Tanji, H., Ohto, U., Shibata, T., Miyake, K. & Shimizu, T. Structural reorganization of the Toll-like receptor 8 dimer induced by agonistic ligands. *Science* **339**, 1426-1429 (2013).

50. Davila, S. *et al.* Genetic association and expression studies indicate a role of toll-like receptor 8 in pulmonary tuberculosis. *PLoS Genet* **4**, e1000218 (2008).

51. Dowling, D.J. *et al.* Toll-like receptor 8 agonist nanoparticles mimic immunomodulating effects of the live BCG vaccine and enhance neonatal innate and adaptive immune responses. *J Allergy Clin Immunol* (2017).

52. Dowling, D.J. *et al.* TLR7/8 adjuvant overcomes newborn hyporesponsiveness to pneumococcal conjugate vaccine at birth. *JCI Insight* **2**, e91020 (2017).

53. Wille-Reece, U. *et al.* HIV Gag protein conjugated to a Toll-like receptor 7/8 agonist improves the magnitude and quality of Th1 and CD8+ T cell responses in nonhuman primates. *Proc Natl Acad Sci U S A* **102**, 15190-15194 (2005).

54. Colditz, G.A. *et al.* Efficacy of BCG vaccine in the prevention of tuberculosis. Meta-analysis of the published literature. *JAMA* **271**, 698-702 (1994).

55. Achkar, J.M. & Casadevall, A. Antibody-mediated immunity against tuberculosis: implications for vaccine development. *Cell Host Microbe* **13**, 250-262 (2013).

56. Skogmar, S. *et al.* CD4 cell levels during treatment for tuberculosis (TB) in Ethiopian adults and clinical markers associated with CD4 lymphocytopenia. *PLoS One* **8**, e83270 (2013).

57. Kumar, N.P. *et al.* Decreased frequencies of circulating CD4(+) T follicular helper cells associated with diminished plasma IL-21 in active pulmonary tuberculosis. *PLoS One* **9**, e111098 (2014).

58. Li, L. *et al.* Mycobacterium tuberculosis-Specific IL-21+IFN-gamma+CD4+ T Cells Are Regulated by IL-12. *PLoS One* **11**, e0147356 (2016).

59. Pulendran, B., Oh, J.Z., Nakaya, H.I., Ravindran, R. & Kazmin, D.A. Immunity to viruses: learning from successful human vaccines. *Immunol Rev* **255**, 243-255 (2013).

60. Fairbairn, L., Kapetanovic, R., Sester, D.P. & Hume, D.A. The mononuclear phagocyte system of the pig as a model for understanding human innate immunity and disease. *J Leukoc Biol* **89**, 855-871 (2011).

61. Landers, T.F., Cohen, B., Wittum, T.E. & Larson, E.L. A review of antibiotic use in food animals: perspective, policy, and potential. *Public Health Rep* **127**, 4-22 (2012).

62. Helbig, E.T., Opitz, B. & Sander, L.E. Adjuvant immunotherapies as a novel approach to bacterial infections. *Immunotherapy* **5**, 365-381 (2013).

63. Brahmakshatriya, V. *et al.* IL-6 Production by TLR-Activated APC Broadly Enhances Aged Cognate CD4 Helper and B Cell Antibody Responses In Vivo. *J Immunol* **198**, 2819-2833 (2017).

64. Havenar-Daughton, C. *et al.* Direct Probing of Germinal Center Responses Reveals Immunological Features and Bottlenecks for Neutralizing Antibody Responses to HIV Env Trimer. *Cell Rep* **17**, 2195-2209 (2016).

65. Havenar-Daughton, C. *et al.* Cytokine-Independent Detection of Antigen-Specific Germinal Center T Follicular Helper Cells in Immunized Nonhuman Primates Using a Live Cell Activation-Induced Marker Technique. *J Immunol* **197**, 994-1002 (2016).

66. Lee, B.R. *et al.* Combination of TLR1/2 and TLR3 ligands enhances CD4(+) T cell longevity and antibody responses by modulating type I IFN production. *Sci Rep* **6**, 32526 (2016).

67. Martins, K.A. *et al.* Adjuvant-enhanced CD4 T Cell Responses are Critical to Durable Vaccine Immunity. *EBioMedicine* **3**, 67-78 (2016).

68. Poteet, E. *et al.* Toll-like receptor 3 adjuvant in combination with virus-like particles elicit a humoral response against HIV. *Vaccine* **34**, 5886-5894 (2016).

69. Soni, C. *et al.* B cell-intrinsic TLR7 signaling is essential for the development of spontaneous germinal centers. *J Immunol* **193**, 4400-4414 (2014).

70. Chakarov, S. & Fazilleau, N. Monocyte-derived dendritic cells promote T follicular helper cell differentiation. *EMBO Mol Med* **6**, 590-603 (2014).

71. Heil, F. *et al.* Species-specific recognition of single-stranded RNA via toll-like receptor 7 and 8. *Science* **303**, 1526-1529 (2004).

72. Hochrein, H. *et al.* Interleukin (IL)-4 is a major regulatory cytokine governing bioactive IL-12 production by mouse and human dendritic cells. *J Exp Med* **192**, 823-833 (2000).

73. de Beaucoudrey, L. *et al.* Revisiting human IL-12Rbeta1 deficiency: a survey of 141 patients from 30 countries. *Medicine (Baltimore)* **89**, 381-402 (2010).

74. Picard, C. *et al.* Clinical features and outcome of patients with IRAK-4 and MyD88 deficiency. *Medicine (Baltimore)* **89**, 403-425 (2010).

75. Ma, C.S. *et al.* Functional STAT3 deficiency compromises the generation of human T follicular helper cells. *Blood* **119**, 3997-4008 (2012).

76. Ma, C.S. *et al.* Monogenic mutations differentially affect the quantity and quality of T follicular helper cells in patients with human primary immunodeficiencies. *J Allergy Clin Immunol* **136**, 993-1006 e1001 (2015).

77. Rao, D.A. *et al.* Pathologically expanded peripheral T helper cell subset drives B cells in rheumatoid arthritis. *Nature* **542**, 110-114 (2017).

.

741
742

Materials and Methods

Cell isolation and culture

Human monocytes, T cells and B cells used in this study were either freshly isolated from peripheral venous blood of healthy volunteers or from buffy coats obtained from the German Red Cross Blood Transfusion Service, Berlin, Germany. Permission for experiments with human primary cells was obtained from the local ethic committee. Peripheral blood mononuclear cells (PBMC) were isolated by density gradient centrifugation over Histopaque-1077 (Sigma-Aldrich; Steinheim, Germany). $CD14^+CD16^-$ monocytes were purified by negative selection via immunomagnetic separation using EasySep monocyte isolation kits with CD16 depletion (Stemcell Technologies; Grenoble, France) according to the manufacturer's instructions. Isolated monocytes were cultured at a density of 1×10^6 cells/ml in RPMI1640 supplemented with 10% fetal calf serum (FCS), 1% glutamine, 1% HEPES buffer, 1% non-essential amino acids (all from Sigma-Aldrich). T cells were cultured in RPMI1640 supplemented with 10% human serum (from the respective T cell donor), 1% glutamine, 1% HEPES buffer, 1% non-essential amino acids, some T cell conditions were supplemented with 2,5ng/ml of TGF-β (eBioscience, San Diego, CA). All cells were grown at 37°C, 5% CO_2 in a humidified incubator.

Untouched human $CD1^+$ mDC were purified by negative selection via immunomagnetic bead separation (Miltenyi Biotec, Bergisch Gladbach, Germany) following the manufacturer's instructions.

Naïve $CD4^+$ T cells were purified by immunomagnetic separation using negative selection (MagniSort™ Human CD4 Naïve T cell Enrichment Kit, eBioscience, San Diego, CA). Total $CD4^+$ T cells (used in Figure 3A, B and D, and Fig. 4F and G and fig. S3) were isolated by magnetic separation using negative selection (MagniSort™ Human CD4 T cell Enrichment Kit, eBioscience).

Untouched naïve human B cells were isolated by immunomagnetic bead separation (Miltenyi Biotec, Bergisch Gladbach, Germany) following the manufacturer's instructions.

Cell purity was routinely checked by flow cytometry and only purities of >85% (monocytes) and >95% (T and B) cells were used for subsequent experiments.

Bacteria and infection

Escherichia coli K12, strain DH5α, thymidine auxotrophs (*thyA*$^{-}$) were selected as previously described[4]. Auxotrophy was confirmed by inoculation and overnight culture of single colonies in LB medium. *ThyA*$^{-}$ *E. coli* (hereafter referred to as EC) grew only in the presence of thymidine and were resistant to trimethoprim. For phagocytosis experiments, EC were grown to mid-log phase, washed twice in phosphate buffered saline (PBS) to remove thymidine and LB salts before addition to cells. For heat killing, EC were grown to log phase, washed and re-suspended in PBS at an optical density at 600nm (OD600) of 0.6, and subsequently incubated at 60 °C for 90 min. Heat-killed *thyA*$^{-}$*E. coli* (HKEC) were used immediately after killing or stored at -80 °C for up to three months. Efficient killing was confirmed by overnight plating on thymidine/trimethoprim-supplemented LB-agar plates. Alternatively, *Bacillus subtilis* strain 168 was used for analogous infection experiments. For heat killing, *B. subtilis* were grown to mid-log phase, washed and re-suspended in PBS at an optical density at 600nm (OD 600) of 0.6, and subsequently incubated at 95°C for 30min. Efficient killing was confirmed by overnight plating on LB-agar plates. . For heat killing, *S. enterica* serovar Typhimurium were grown to mid-log phase, washed and re-suspended in PBS at an optical density at 600nm (OD 600) of 0.6, and subsequently incubated at 95°C for 30min. Efficient killing was confirmed by overnight plating on LB-agar plates. Infection of human monocyte was performed at the indicated multiplicities of infection (MOI).

BCG was grown in Middlebrook 7H9 medium supplemented with 0.05% Tween 80. For phagocytosis experiments, BCG were grown to mid-log phase, washed once in phosphate buffered saline (PBS) and resuspended in complete cell culture media via repeated tuberculin type needle passages (10x). For heat killing, BCG were grown to log phase and incubated at 60°C for 90min. Heat-killed BCG (HKBCG) were used immediately after killing. Efficient killing was confirmed by 96h inoculation in competent media.

Co-culture assays

For monocyte : T cell co-cultures monocytes were cultured as described above and stimulated as indicated (e.g. EC, HKEC MOI 1-25) in antibiotic-free medium. After one and a half hours, penicillin/streptomycin (1%) was added together with autologous naïve CD4^{+} T cells at a monocyte to T cell ratio of 2:1 and staphylococcal enterotoxin B (SEB, Sigma) at a concentration of 1.0µg/ml. After 5 days of co-culture T cells were harvested, washed, restimulated with Phorbol-

12-myristat-13-acetat (PMA, 50ng/ml) and Ionomycin (1µg/ml, both obtained from Sigma), stained and analyzed by flow cytometry.

For T : B cell co-cultures, T cells were differentiated by co-cultures with autologous monocytes for 6 days as described before. $CXCR5^{+}ICOS^{+}PD\text{-}1^{hi}$ T cells were sorted by flow cytometry (BD FACS-Aria II) and added to naïve autologous B cells at a T to B cell ratio of 1:2 in the presence of SEB (1µg/ml). After 12 days co-culture B and T cells were harvested and analyzed by flow cytometry. For analysis of plasma blast differentiation, sorted T_{FH} ($CD19^{-}$ $CD4^{+}$ $CD45RA^{-}$ $CXCR5^{+}$) or naive ($CD19^{-}$ $CD4^{+}$ $CD45RA^{+}$) T cells were cocultured with memory B cells at a ratio of 1:1 in the presence of 4 ng/ml SEB for 7 days.

Antibodies and reagents

Antibodies for flow cytometry: CD3 (UCHT1, cat.: 300415), CD4 (OKT4, cat.: 317424), IFNy (4S.B3, cat.: 502528), IL17 (BL168, cat.: 512306), CXCR5 (J252D4, cat.: 356904), PD1 (EH12.2H7, cat.: 329922), ICOS (C398.4A, cat.: 313510), CD19 (HIB19, cat.: 302228 or SJ25C1, cat.: 363022), CD20 (2H7, cat.: 302324), CD27 (O323, cat.: 302810), CD38 (HIT2, cat.: 303516 or or M-T271, cat.: 356418), IgM (MHM-88, cat.: 314520), IgD (IA6-2, cat.: 348216), MHC2 (L243, cat.: 307610), anti IL-1b (H1B-27, cat.: 511604), Zombie violet (cat.: 423113;(all from Biolegend, San Diego, CA). Anti IFNar (polyclonal , cat.: ab10739, Abcam, Cambridge, UK), BCL6 (K112-91, cat.: 561522/ 561525, BD, Franklin Lake, NJ), IL-21 (ebio3A3-N2, cat.: 50-7219, eBioscience), CD14 (TÜK4, cat.: 130-096-875, Miltenyi Biotec, Bergisch Gladbach, Germany), CD38 (OKT 10, CRL-8022, ATCC, Manassas, VA).porcine Monocyte/Granulocyte (74-22-15A, cat.: 561499, BD, Franklin Lake, NJ), porcine CD3 (BB23-8E6-8C8, cat.: 561478), porcine CD4 (74-12-4-RUO, cat.: 561472, BD), porcine CD8b (295/33-25, cat.: 561484, BD), IL-21 (polyclonal, cat.: orb9043, Biorbyt, San Francisco, CA) porcine CD8a (76-2-11, cat.: 561475, BD), porcine CD2 (MSA4, cat.: WS0590S-100, Kingfischer Biotech), porcine SLA Class II DR (2E9/13, cat.: MCA2314F, AbD Serotec), porcine CD21 (BB6-11C9.6, cat.: SBA-4530-09, Southern Biotech), porcine TCR1 δ (PGBL22A, cat.: WS0621S-100, Kingfischer Biotech), mouse-IgG (Poly4053, cat.: 405317, Biolegend), porcine IgM (polyclonal, cat.: AAI48B, Bio-Rad), Streptavidin (cat.: 25-4317-82, eBioscience), Foxp3 (FJK-16s, cat.: 48-5773-82, eBioscience), Tbet (eBio4B10, cat.: 12-5825-82, eBioscience). Fixable Viability Dyes (cat.: 65-0865-14 and 65-0866-14, eBioscience).

Neutralizing antibodies: anti-IL-6 (6708, cat.: MAB206-SP, R&D Systems, Minneapolis, MN), anti-IL-12 (B-T21, cat.: BMS152, eBioscience) and anti-TNFα (MAb11, cat.: 502901, Biolegend) were used at 10µg/ml. Anti-IL-27 (307426, cat.: MAB25261 F, R&D Systems) was used at 5µg/ml.

Recombinant cytokines: rIL-12 (eBioscience) was used at 100pg/ml, rTNF, rIL-6 (eBioscience), rIL-27 (R&D Systems) were used at 10 ng/ml.

TLR ligands were purchased from Invivogen (Toulouse, France) and used at the indicated concentration: CL075 (3M002; 1µg/ml), LPS-EK Ultrapure (2µg/ml), Pam3CSK4 (200ng/ml), Poly(I:C) LMW (2µg/ml), ODN 2395 (5µM). Bacterial RNA was isolated from mid-log phase cultures of DH5alpha *E. coli* using Trizol (Life Technologies, Karlsruhe, Germany). Transfection of bacterial RNA into human monocytes was performed using polycationic polypeptide poly-L -arginine (pLa) (Sigma-Aldrich).

Enzyme-linked immunosorbent assay (ELISA)

TNF, IL-1β, IL-6, IL-10, IL-12p40, IL-23, GM-CSF and IL-27 concentrations in culture supernatants were measured by ELISA (all purchased from eBioscience) according to standard manufacturer's recommendations. Concentrations of IL-12p70 were measured using human IL-12p70 High Sensitivity ELISA kit (eBioscience). The samples were analyzed for absorbance at 450 nm using FilterMax F5 Multi-Mode Microplate Reader (Molecular Devices, Biberach an der Riss, Germany). Porcine IL-12p40 and IL-6 concentrations in culture supernatants were measured by ProcartaPlex Pig Kit (eBioscience) or by Quantikine ELISA kit (R&D Systems) and results were collected using a Luminex MAGPIX instrument (Merck Millipore, Billerica, MA). Human IgG was determined by ELISA using polyclonal goat anti-human IgG (TAGO Immunologicals, Burlingame, CA) and purified human IgG as standard. Results were collected on a Spark multimode reader (Tecan, Männedorf, Switzerland).

Anti-S. enterica IgG ELISA

96-well microtiter plates were coated overnight with *S. enterica* serovar Typhimurium (Salmoporc-STM) lysates (3µg/ml) that we generated from log-phase cultures of *Hys⁻Ade⁻ S. enterica*. Serum samples from immunized pigs were serially diluted (12 dilutions) and incubated in the pre-coated plates for 12 h at 4 °C followed by washing and incubation with goat anti-pig IgG (gamma)-HRP (SeraCare Life Sciences, Milford, MA) for 1 h. Bound goat anti-pig IgG (gamma)-

HRP was visualized by the addition of TMB substrate (Thermo Fisher), and the anti-*S. enterica* antibody titers for each animals were visualized as absorbance readings at 450nm at a set serum dilution of 1 to 51200.

RNA Isolation

$CD14^{+}CD16^{-}$ human monocytes were sorted by flow cytometry and were infected with EC at MOI=10 or stimulated with HKEC at 10:1 ratio of bacteria to cells. After 6 hours, cells were harvested, washed once in PBS, and lysed in Trizol (Life Technologies). Total RNA was prepared according to the manufacturer's suggested protocol.

Gene Array

Total RNA was prepared from four independent experiments (= four separate donors) according to the Trizol manufacturer's protocol. Samples were further purified on columns (RNeasy Micro Kit, Qiagen, Hilden, Germany).

RNA integrity was checked on an Agilent 2100 Bioanalyser (Agilent Technologies, Santa Clara, CA) with 6000 Nano Chips. RNA was judged as suitable only if samples showed intact bands of 18S and 28S ribosomal RNA subunits, displayed no chromosomal peaks or RNA degradation products, and had a RNA integrity number (RIN) above 8.0.

One-hundred nanograms of RNA were used for whole-transcript cDNA synthesis with the Ambion WT expression kit (Life Technologies). Hybridization, washing and scanning of an Affymetrix GeneChip Human Gene 1.1 ST 24-array plate was carried out according to standard Affymetrix protocols on a GeneTitan instrument (Affymetrix, Santa Clara, CA).

Quality control, normalization and statistical analysis was performed using MADMAX, a pipeline consisting of integrated Bioconductor packages[78]. Probe sets were redefined according to Dai *et al.* using current genome information[79]. Normalized gene expression estimates were obtained from the raw intensity values by using the robust multiarray analysis preprocessing algorithm available in the library "AffyPLM" using default settings[80]. Only genes that were targeted by at least 7 probes, reached log2 expression level of>4.32 on at least three microarrays and had a log2 interquartile range value >0.25 across all samples were considered for further analysis. Intensity-based moderated t-statistics were applied for pairwise comparisons to identify differentially

890 regulated genes[81]. To correct for multiple testing a false discovery rate method was used to
891 calculate q-values[82]. A q-value < 0.01 was considered significant.

892 *RNA interference*

893 Silencer Select siRNA duplexes targeting TLR8 (sequence ID: s27920, s27921 and s27922),
894 MyD88 (sequence ID: s9136, s9137 and s9138) and negative controls were obtained from Life
895 Technologies. Monocytes cultured in 96-well plates were transfected with 25nM of each siRNA
896 using Viromer Blue transfection reagent (Lipocalyx, Leipzig, Germany) following manufacturer
897 recommendations for sensitive cells and reverse transfection. Cells were plated at a density $5x10^5$
898 cells/ml in a final volume of 100µl in 96 well plates. Forty-eight hours post transfection cells were
899 infected or treated as described. Knockdown of TLR8 and Myd88 was confirmed 48 hours after
900 siRNA transfection by RT-PCR using specific primers (TLR8: forward primer 5′-
901 AgTTTCTCTTCTCggCCACC-3′ and reverse primer, 5′-ACATgTTTTCCATgTTTCTgTTgT -3′,
902 MyD88: forward primer 5′-TCTCCAggTgCCCATCAgAA-3′ and reverse primer 5′-
903 ggTTggTgTAgTCgCAgACA-3′).

904 Four Custom designed Silencer Select siRNA duplexes targeting porcine TLR8 (combination of
905 four siRNA duplexes) were purchased from Life Technologies with sequences:

906 TLR8-1 sense: 5´-GCAAAUUGAUUUUACCAUUTT-3′;

907 antisense: 5´-AAUGGUAAAAUCAAUUUGCTT-3′;

908 TLR8-2 sense: 5´-GAUUUAAGCUUGAACAGUATT-3′;

909 antisense: 5´-UACUGUUCAAGCUUAAAUCTA-3′;

910 TLR8-3 sense: 5´-GCAUCUUUACUUUAACAGATT-3′;

911 antisense: 5´-UCUGUUAAAGUAAAGAUGCTG-3′;

912 TLR8-4 sense: 5´-CAAUAUUCGUUUUAACCAATT-3′;

913 antisense: 5´-UUGGUUAAAACGAAUAUUGTC-3′;

914 Porcine $CD14^+$ monocytes cultured in 96-well plates were transfected with 25nM of each siRNA
915 folloing the protocol desctribed above for human cells. Forty-eight hours post transfection cells
916 were infected or treated as described.

Flow cytometry and cell sorting

Flow cytometry regularly was performed on a BD FACS Canto II cytometer Data was analyzed using FlowJo software (Treestar, San Carlos, CA).

$CD14^+CD16^-$ monocytes were sorted from PBMCs on a BD Aria II SORP cell sorter (BD Biosciences) $CD4^+CXCR5^+$ and $CD4^+CXCR5^-$ T cells were sorted from monocyte : T cell co-cultures on a BD Aria II SORP cell sorter. In vitro generated Tfh cells were sorted on an ARIA II sorter as $CD19^-$ $CD4^+$ $CD45RA^-$ $CXCR5^+$ and naive T cells as $CD19^-$ $CD4^+$ $CD45RA^+$. Memory B cells were sorted from human tonsils as $CD4^-$ $CD19^+$ IgD^- $CD38^-$ cells. Cell purity checks were performed and a purity of >97% was confirmed.

QuantiGene Plex transcript analysis

Quantigene multiplex-plex assay (Affymetrix,) was performed to quantify the expression of the following genes *GATA3*, *MAF*, *IL21*, *TBX21*, *RORC*, *FOXO1*, *BCL6* and two housekeeper genes (*ACTB* and *HPRT1*) according to the manufacturer's protocol. In brief, $CD4^+$ T cells were lysed at a concentration of 500 cell/µl of lysis mixture supplemented with proteinase K and incubated at 50°C for 30 min, prior to addition to a hybridization plate. The hybridization plate was sealed with heat-sealing foil and placed in a shaking incubator (VorTemp 56) at 54±1°C and 600 rpm to allow the samples to hybridize for 18-22 h. Fluorescent bead signal detection was obtained using Bio-Plex Suspension Array System (Bio-Rad Laboratories, Hercules, CA). The mean fluorescent intensity for each probe was recorded.

Animal experiment

The animal experiments were performed in accordance with the Danish Animal Welfare Act under approval and authorization issued by the Danish Animal Experiment Inspectorate.

In total, 18 five-week-old pigs (Danish Landrace/Danish Yorkshire crossbreeds, paternal lineage Duroc) of both sexes, raised on a commercial farm (Bøgekærgård, Faxe, Denmark) were stratified by size (6.3 to 10.4 kg, averaging 8.0 kg) and sex, and distributed to three groups. Animals in each group received 1 ml subcutaneous vaccination in the right side of the neck as follows: 1) live *Salmonella enterica* serovar Typhimurium vaccine (Salmoporc STM Ch.-B. 022 07 15, IDT Biologika, Dessau-Roßlau, Germany) containing 3.32 x 10^8 CFU per dose, according to the product insert); 2) heat-inactivated (65° for 90 minutes) Salmoporc STM vaccine (HKST) using

the same dose as in 1); 3) saline alone. The live vaccine was administered within 2h of reconstitution. The same immunization regimen was repeated as booster injections on day 14. Heat-killing of the vaccine was confirmed by absence of bacterial growth on LB plates incubated at 37°C for 24h. Throughout the experiment the pigs were housed in two adjoining boxes equally mixed across the 3 treatment groups. One pig in the live vaccine group was euthanized on day 19 of the experiment due to severe umbilical hernia, unrelated to the vaccine. One pig in the control group presented on day 0 of the experiment with fever, dyspnea and generalized fatigue, suspected of pneumonia, and was therefore treated successfully with 160 mg benzylpenicillin and 200 mg dihydrostreptomycin (0.8 ml Streptocillin Vet) over 3 consecutive days. It was excluded from the analysis. Five animals per group were included in the final analyses.

Animals were sacrificed according to regulations. Transverse sections of spleen and prescapular lymph node (LN, *cervicalis superficialis dorsalis*) draining from the injection site were fixated in 10% neutral-buffered formalin (4% formaldehyde, Pioneer Research Chemicals Ltd) for immunohistochemistry. The remaining LN and spleen tissues samples were homogenized using disposable scalpels and single-cell suspensions were isolated by forcing homogenized tissue samples through a cell strainer (70 µm, Greiner Bio-One, Kremsmünster, Austria), followed by two washes with RPMI 1640 and subsequently cultured in RPMI1640 supplemented with 10% fetal calf serum (FCS), 1% glutamine, 1% HEPES buffer, 1% non-essential amino acids (all from Sigma-Aldrich).

For BCG vaccination 12 female pigs (Danish Landrace/Danish Yorkshire crossbreds and paternal Duroc) were delivered after weaning to the research facilities at the National Veterinary Institute, Technical University of Denmark, Frederiksberg, Denmark from a commercial farm (Askelygård, Roskilde, Denmark). At 5 weeks of age the pigs were stratified by size (total weight range 5.5-11.5 kg, mean 8.9 kg) and allocated to two vaccination groups, receiving either 1.5-2 vials of BCG (Statens Serum Institut, Copenhagen, Denmark) resuspended in 0.8ml Sauton diluent (~15-20 times a standard BCG dose) or 1.0ml Sauton diluent alone, applied by three adjacent injections s.c. in the right hind leg by a midwife with extensive experience in BCG vaccination of human newborns. 24 days after vaccination, venous blood was collected into EDTA containing tubes, the pigs were sacrificed according to regulations, and the spleens were retrieved and preserved in cold

RPMI-1640 Glutamax supplemented with penicillin and streptomycin (all Gibco, city, country) for subsequent processing.

For *in vitro* experiments reported in Fig. 7 and Supplementary Figure 4 spleens samples were collected from German Landrace pigs of both sexes aged between 8 weeks and 1 year. Single cell suspensions were prepared as described above.

Splenocytes were cultured in IMDM (Pan-biotech, Aidenbach, Germany) supplemented with 10% FCS and stimulated with ST, HKST (MOI 0.1, 0.5, 1, 3), LPS (2µg/ml), CL075 (1µg/ml) or pLa+RNA (280ng and 237ng respectively) in the presence of Concavalin A (2µg/ml) (Fisherscientific, Schwerte, Germany). After one hour penicillin/streptomycin (1%) was added. After 4 days cells were restimulated with Phorbol-12-myristat-13-acetat (PMA, 50ng/ml) and Ionomycin (1µg/ml, both obtained from Sigma) and then harvested, washed and analyzed by flow cytometry. Live and dead cells were discriminated using Zombie Violet Fixable Viability Kit (Biolegend), dead cells were excluded from the analysis.

Immunohistochemistry

Spleen samples were immersion-fixed in formalin and embedded in paraffin, cut in 2 µm sections for immunohistochemical analyses after dewaxing in xylene and rehydration in decreasing ethanol concentrations. For detection of PAX5, KI67 and BCL22, heat-mediated antigen retrieval was performed in 10 mM citric acid (pH 6.0), microwaved at 600 W for 12 min. Spleen sections were incubated with a purified mouse antibody monoclonal to PAX5 (1:400, clone 24/Pax5, BD Biosciences, Heidelberg, Germany) or BCL2 (1:100, LS-B2352, LSBio, Seattle, WA, USA) or with a purified rabbit antibody monoclonal to KI67 (1:150, clone SP6, Cell Marque, Rocklin, CA, USA) at 4°C overnight. Incubation with an irrelevant immuno-purified mouse or rabbit antibody at the same dilution served as negative controls. Slides were incubated with biotinylated, secondary goat anti-mouse IgG (1:200, BA 9200, Vector Burlingame, CA) or goat anti-rabbit IgG (1:200, BA 1000, Vector, Burlingame, CA) antibodies and HRP-coupled streptavidin. Diaminobenzidine (DAB) was used as substrate for color development. All slides were counterstained with hematoxylin, dehydrated through graded ethanols, cleared in xylene and coverslipped. Whole slide

images of spleen tissues were generated by Aperio CS2 digital pathology scanner (Leica Biosystems Imaging Inc., Vista, CA, USA).

Immunoflourescence

For immunofluorescent co-staining of PAX5 and KI67, slides were incubated with the purified mouse antibody monoclonal to PAX5 (1:50) over night at 4°C as described above and with Alexa Fluor 568-conjugated, secondary goat anti-mouse IgG antibody (1:200, Thermo Fisher Scientific, Darmstad, Germany) for 45 min. at room temperature. Slides were then incubated with a purified rat antibody monoclonal to KI67 (1:100, clone SolA15, eBioscience) at 4°C over night, incubated with Alexa Flour 488-conjugated, secondary goat anti-rat IgG antibody (1:200, Thermo Fisher Scientific) for 45 min. at room temperature and mounted with Roti-Mount Fluor-Care DAPI (4,6-diaminidino-2-phenylindole, Carl Roth, Karlsruhe, Germany). Adequate negative controls, including incubation of slides with only one primary but both secondary antibodies, were conducted. Slides were analyzed by immunofluorescence microscopy with an Olympus BX41 microscope equipped with a DP80 camera (Olympus, Hamburg, Germany).

Case-Control Study

Samples of TB patients and healthy volunteers were collected in Mahavir Hospital, Hyderabad (India) and the generated cohort has been described before [83]. Informed consent was obtained from all individuals, and all investigations were conducted according to the principles of the Helsinki Declaration. Written approval was obtained from the research ethics board of the Central University of Hyderabad and Mahavir Hospital. Patients were enrolled in the Revised National Tuberculosis Control Program (RNTCP) of India, and recruited into the study on the day of treatment initiation (according to DOTS strategy). HIV-positive and relapse cases were excluded from the cohort. TB diagnosis was based on clinical examination, chest X-Ray, positive sputum test or histopathology. Healthy household contacts of the TB patients were recruited as controls, to ensure comparable exposure rates and environmental conditions. BCG vaccination status was determined by the presence of a BCG-related skin scar. The cohort consisted of 293 patients and 165 controls. 61,4% of the TB patients had pulmonary TB (PTB) and 38.6% extra-pulmonary TB (ETB). Controls were significantly older (mean=34.2±9.3) than patients (mean=25.4±10,4;$t(456)=8.787$;$p<0.0001$) and had a significantly higher mean BMI (mean=23.8±4.9 and mean=18.0±4.1 respectively, $t(292.8)=12.995$;$p<.0001$). Gender distribution did not differ significantly between

controls (59.4% females) and patients (61.8% females). The age and BMI differences were corrected for using a binary logistic regression model.

SNP Analysis

DNA of all study subjects was extracted from buccal swabs using FlexiGene DNA extraction Kit (Qiagen). TLR8 SNPs were analyzed by real-time PCR on a Light Cycler instrument (Roche, Mannheim, Germany) using the following PCR primer sets:

forward 5'-TCAGGAAGTTAGCCAGTTTCTC-3',

reverse 5'-CCTGCATTTACAGTTGTTTCGAT-3',

sensor 5'-AAATAGAAGTGGCTTACCACGTTTCTG-3'T-FITC,

anchor Cy5-5'-TTCTAATTTTTCATTCCGTAACTTGCAGCAGCGCA-3'.

Based on previous observations that the presence of an A defines the functionality, we defined the A/AA/AG as TLR8-A, and G/GG as TLR8-G status for our analysis.

Statistical Analysis

Statistical analyses of in vitro experiments were performed using one-way-ANOVA test and Holm-Sidak's multiple comparisons test, or 2way-ANOVA, or Wilcoxon's matched-pairs signed rank test, or linear regression analysis where appropriate. Calculations were performed using GraphPad Prism 6 Software (GraphPad Software, La Jolla, CA, USA)

For all statistical analysis a p-value <0.05 was considered statistically significant. 95% Confidence Intervals are given in squared brackets in tables S3-S4 [CI 95%]. Baseline characteristics of the study population were analyzed using student's t-test or Pearson's chi-squared (χ^2) test. TLR8 allele frequencies were compared using binary logistic regression, summarizing recessive genotypes and adjusting for age, BMI and gender. Interaction between BCG and TLR8-A/G was assessed using Wald's statistics. Statistical tests were performed using IBM SPSS Statistics 21 software and figures were generated using GraphPad Prism 6 Software.

Supplementary References

78. Lin, K. *et al.* MADMAX - Management and analysis database for multiple ~omics experiments. *J Integr Bioinform* **8**, 160 (2011).

79. Dai, M. *et al.* Evolving gene/transcript definitions significantly alter the interpretation of GeneChip data. *Nucleic Acids Res* **33**, e175 (2005).

80. Irizarry, R.A. *et al.* Exploration, normalization, and summaries of high density oligonucleotide array probe level data. *Biostatistics* **4**, 249-264 (2003).

81. Sartor, M.A. *et al.* Intensity-based hierarchical Bayes method improves testing for differentially expressed genes in microarray experiments. *BMC Bioinformatics* **7**, 538 (2006).

82. Storey, J.D. & Tibshirani, R. Statistical significance for genomewide studies. *Proc Natl Acad Sci U S A* **100**, 9440-9445 (2003).

83. Dittrich, N. *et al.* Toll-like receptor 1 variations influence susceptibility and immune response to Mycobacterium tuberculosis. *Tuberculosis (Edinb)* **95**, 328-335 (2015)

Figure legends

Fig. 1. Innate immune recognition of live but not dead bacteria promotes T_H1 and T_{FH} differentiation. (**a**) Human monocytes were stimulated with medium (ctrl), live *E. coli* (EC) or heat killed *E. coli* (HKEC) and co-cultured with autologous naïve $CD4^+$ T cells in the presence of SEB (TCR stimulus in all T cell conditions). Proliferation (CFSE-dilution) and cytokine production was measured on day 5. (**b**) Quantification of cytokine-positive $CD4^+$ T cells. Each dot represents an independent experiment / donor (n=9, 9, 7). (**c,d**) Expression of CXCR5, ICOS, PD-1 was measured by flow cytometry (c), and quantified (d) (n=13). (**e-f**) Similar experiment as in (a), expression of BCL6 and IL-21 was measured by flow cytometry (n=9), and quantified (f). (**g**) Similar experiment as in all other panels using mDC-1 as APC (n=3). (**h**) Quantification of (g). (**i**) Expression of the indicated genes was measured in $CD4^+$ T cells at the indicated time points by fluorescent hybridization-based multiplex assay. Results are expressed as corrected fluorescence intensity (FI) minus FI in ctrl samples at the same time point (n=6). Error bars are mean ± SEM (**; p<0.01, ***; p<0.001; ****; p<0.0001).

Fig. 2. *De novo* generated T_{FH} cells interact with and help B cells. (**a**) $CD4^+$ T cells were co-cultured with APC as in Fig. 1a and added to autologous naïve B cells after 5 days. T_{FH} cell markers were measured after 12 days of sequential co-culture (n=2). (**b-d**) sorted $CD4^+CD45RA^-CXCR5^+$ T_{FH} cells and sorted autologous naïve $CD4^+CD45RA^+$ T cells were co-cultured with tonsillar memory B cells for 7 days and generation of $CD38^+CD27^{++}$ plasma cells were measured (b) and quantified (c, n= 9, 9, 3). Culture supernatants were analyzed for IgG production by ELISA (f) (n=9, 9, 3). Error bars are mean ± SEM (*; p<0.05, **; p<0.01)

Fig. 3. Detection of viable bacteria induces transcriptional remodeling and skewed cytokine responses in human monocytes. (**a**) Human $CD14^{+}CD16^{-}$ monocytes (n=4) were stimulated with either medium (ctrl), EC or HKEC for 6h and subjected to genome wide transcriptional analysis. Depicted is the mean signal log ratio (SLR) for each gene in EC vs ctrl treated cells plotted against HKEC vs ctrl treated cells. Red circles indicate genes with SLR difference >2 in EC vs HKEC. (**b**) Heat map of the 193 regulated genes with a fold change >2 or <–2 of four independent experiments/donors. (**c**) Cytokine secretion from APC left untreated (ctrl), or stimulated with EC or HKEC for 18h (n=3-6). (**d**) Cytokine secretion from APC stimulated with increasing multiplicity of infection (MOI) of EC or HKEC (n=4). (**e**) Cytokine secretion from APC stimulated with live or heat killed *B. subtilis* (BS and HKBS respectively, upper panel, n=2-5), and live or heat killed *M. bovis* strain *BCG* (BCG and HKBCG respectively, lower panel, n=4) (**f**) APC were treated as in (c) and surface expression of the indicated markers was measured by flow cytometry at 18h post infection (n=5). Error bars are mean ± SEM (*; $p<0.05$, **; $p<0.01$, ***; $p<0.001$)

Fig. 4. 'Viability-induced' IL-12 production is a critical signal for T_{FH} differentiation. (**a,b**) $CD4^{+}$ T cells were polyclonally activated by plate-bound anti-CD3 and soluble anti-CD28 antibodies in the presence of supernatants collected from APC stimulated for 18h with ctrl, EC or HKEC. Cytokine production was measured by flow cytometry (a, n=19, 8) and ELISA (b, n=11). **(c)** Linear regression analysis of IL-21 production by $CD4^{+}$ T cells and the indicated cytokines in APC supernatants (n=45, 21, 21). (**d-g**) T cells were cultured as in a-c in the presence of the indicated neutralizing antibodies or recombinant cytokines (αIL-12; anti-IL-12 antibody etc., rIL-12: recombinant IL-12 etc.). IL-21 and BCL6 expression were measured by flow cytometry (d,e) (n=8), IL-21 production was quantified by ELISA (f, g) (n=7). Error bars are mean ± SEM (*; $p<0.05$, **; $p<0.01$, ***; $p<0.001$).

Fig. 5. APC sense live bacteria via TLR8. (**a**) Monocytes treated as indicated ('2'; ligand for TLR2 etc.), cytokine production was measured by ELISA (n=2). (**b**) Monocytes were stimulated as indicated (pLA= polycationic polypeptide poly-l-arginine (*pLa*), RNA= bacterial RNA) and cytokine production was measured by ELISA (n=3, 4, 4). (**c-d**) Cytokine release from primary human monocytes treated with siRNA against TLR8 (c) and MyD88 (d) or control siRNA (ctrl) and stimulated as indicated (n=3). #; not detectable. Error bars are mean ± SEM. (**; p<0.01, ***; p<0.001)

Fig. 6. TLR8 is crucial in the detection of viable bacteria and subsequent instruction of T_{FH} responses. (**a-b**) $CD4^+$ T cells were stimulated in the presence of culture supernatants from APC previously stimulated with live or killed bacteria, or the indicated TLR ligands. IL-21 and BCL6 expression were detected by flow cytometry (n=7). (**b**) Quantification of (a). (**c**) APC were stimulated with live or killed bacteria, the TLR8 agonist CL075 (0.1, 0.5 and 1µg/ml respectively), MPLA (0.1, 0.5 and 1µg/ml respectively), or CpG (0.1, 1 and 2.5µM respectively), and subsequently co-cultured with $CD4^+$ T cells as in Figure 1. BCL6/IL-21 expression was detected by flow cytometry (n=7). (**d-e**) APC were stimulated with live or killed bacteria, and/or with bacterial RNA complexed with pLa, and supernatants were used to stimulate $CD4^+$ T cells as in (a). BCL6/IL-21 expression was detected by flow cytometry and IL-21 production was measured by ELISA (n=4). (**f-g**) $CD4^+$ T cells were stimulated in the presence of culture supernatants from siRNA-treated APC (n=8). IL-21/ BCL6 co-expression was measured by flow cytometry (f, g left panel) and IL-21 production was measured by ELISA (g, right panel). Error bars are mean ± SEM. (*; p<0.05, **; p<0.01, ***; p<0.001).

Fig. 7. Detection of viable bacteria in porcine APC promotes T_{FH} differentiation. (**a, b**) Porcine $CD14^+CD172^+$ monocytes (a) and $CD14^-CD172^+$ DC (b) were sorted from spleen samples and stimulated with medium (ctrl), EC, HKEC, live attenuated *S. enterica* serovar Typhimurium vaccine (ST), heat killed ST (HKST) or with CL075. IL-12p40 and IL-6 was measured by multiplex bead array (n=3). (**c**) Cytokine release from porcine splenic $CD14^+$ monocytes treated with siRNA against porcine TLR8 or control siRNA (ctrl), and stimulated as indicated (n=3). (**d**) Porcine splenocytes were stimulated with ConA in the presence of increasing doses of ST or HKST. BCL6/IL-21 expression was measured in $CD4^+$ T cells by flow cytometry on day 4. (**e**) Quantification of (d, n=3). (**f**) Porcine splenocytes were stimulated with CL075, LPS, or bacterial RNA (RNA + pLA) in the presence of ConA. BCL6/IL-21 expression was measured in $CD4^+$ T cells on day 4 (n=3). Error bars are mean ± SEM. (n.s.; not significant, *; $p<0.05$, **; $p<0.01$, ***; $p<0.001$).

Fig. 8 A live attenuated vaccine promotes T_{FH} differentiation *in vivo*. (**a**) Five week old domestic piglets were vaccinated subcutaneously with ST, HKST or saline (ctrl), and BCL6/IL-21 expressing $CD4^+$ T cells were measured in draining lymph nodes (LN) or spleens on day 30 after immunization (n=5/group). (**b**) Quantification of (a). (**c**) Sections of paraffin embedded spleen tissues were stained for PAX5. Scale bars: upper panels = 5 mm; lower panels = 500 µm. (**d**) morphometric quantification of $PAX5^+$ follicles spleen sections tissue represented in (c). (**e**) Co-immunofluorescence staining of PAX5 (red) and KI67 (green) on spleen section of pigs vaccinated with ST. The cell nuclei were stained with DAPI (blue). Scale bar = 50 µm. (**f**) Antibody forming cells (AFC) / plasma cells (PC) were measured by flow cytometry in spleen samples (n= 4/group). (**g**) anti-*Salmonella* IgG was measured by ELISA in serum samples taken before vaccination (day 0), and on day 14 and 21 post-vaccination. Error bars are mean ± SEM. (*; $p<0.05$, **; $p<0.01$).

Fig. 9. Association of a TLR8 SNP with BCG-induced immunity. (**a**) TLR8-A and TLR-G allele distribution in 458 subjects (293 cases of confirmed TB and 165 household contacts = controls) (left panel), and 345 subjects (180 cases of confirmed pulmonary TB (PTB) and 165 controls) (right panel). (**b**) TLR8-A and TLR8-G allele distribution in BCG-vaccinated (upper panel) and unvaccinated (lower panel) PTB cases and controls, one individual was excluded from the analysis due to unclear vaccination status. (**c**) Odds ratio (OR [CI95%], adjusted for sex, age and BMI) for PTB in BCG vaccinated versus unvaccinated subjects calculated for the whole study population and separately for each TLR8 genotype (bars represent OR, error bars represent CI 95%). ORs differ significantly between TLR8-A and TLR8-G as calculated by Wald's test. (*; $p<0.05$, **; $p<0.01$).

Fig. 1

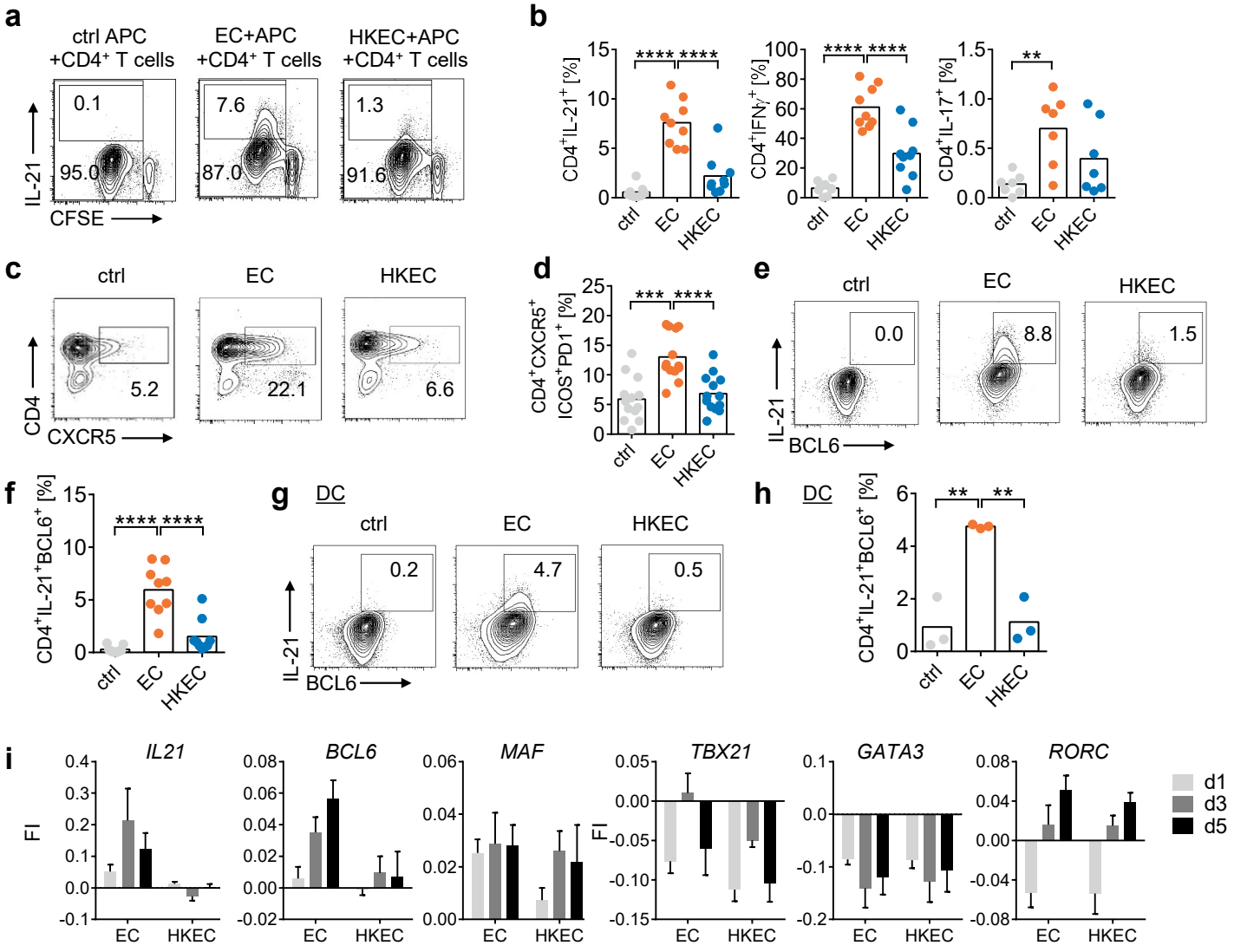
a
ctrl APC +CD4+ T cells
EC+APC +CD4+ T cells
HKEC+APC +CD4+ T cells
0.1
95.0
7.6
87.0
1.3
91.6
IL-21
CFSE
b
CD4+IL-21+ [%]
CD4+IFNγ+ [%]
CD4+IL-17+ [%]
****
**
ctrl
EC
HKEC
c
ctrl
EC
HKEC
5.2
22.1
6.6
CD4
CXCR5
d
CD4+CXCR5+ ICOS+PD1+ [%]
***
****
e
0.0
8.8
1.5
IL-21
BCL6
f
CD4+IL-21+BCL6+ [%]
g
DC
0.2
4.7
0.5
h
i
IL21
BCL6
MAF
TBX21
GATA3
RORC
FI
d1
d3
d5

Fig. 2

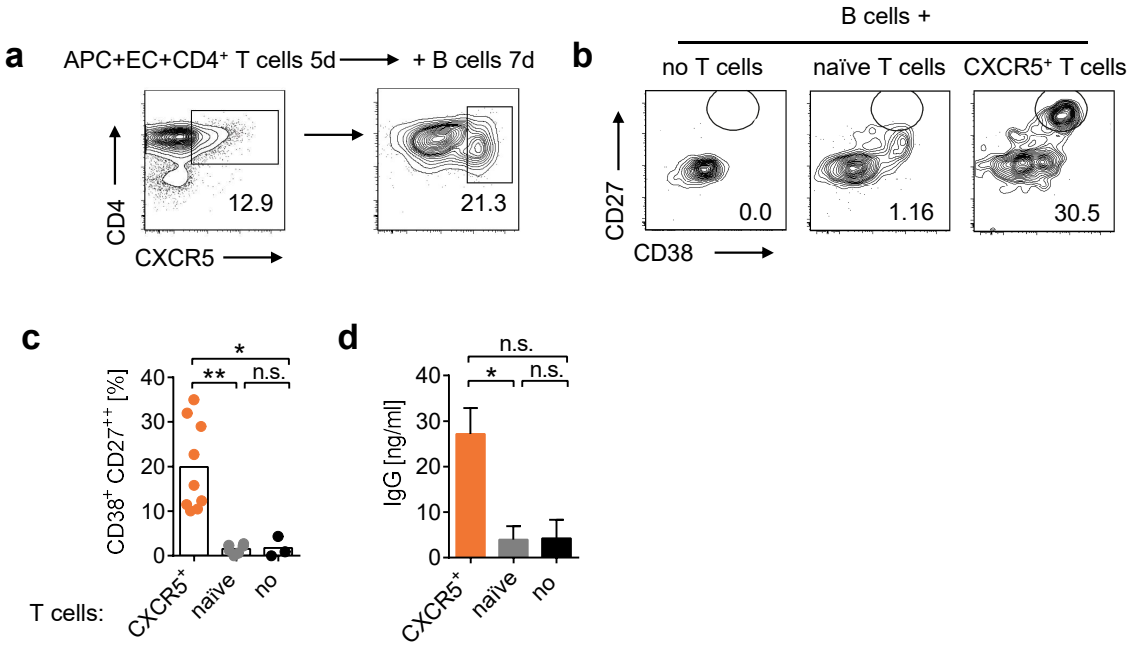
a
APC+EC+CD4⁺ T cells 5d
+ B cells 7d
CD4
CXCR5
12.9
21.3
b
B cells +
no T cells
naïve T cells
CXCR5⁺ T cells
CD27
CD38
0.0
1.16
30.5
c
CD38⁺ CD27⁺⁺ [%]
*
**
n.s.
T cells:
CXCR5⁺
naïve
no
d
IgG [ng/ml]
n.s.
*
n.s.
CXCR5⁺
naïve
no

Fig. 3

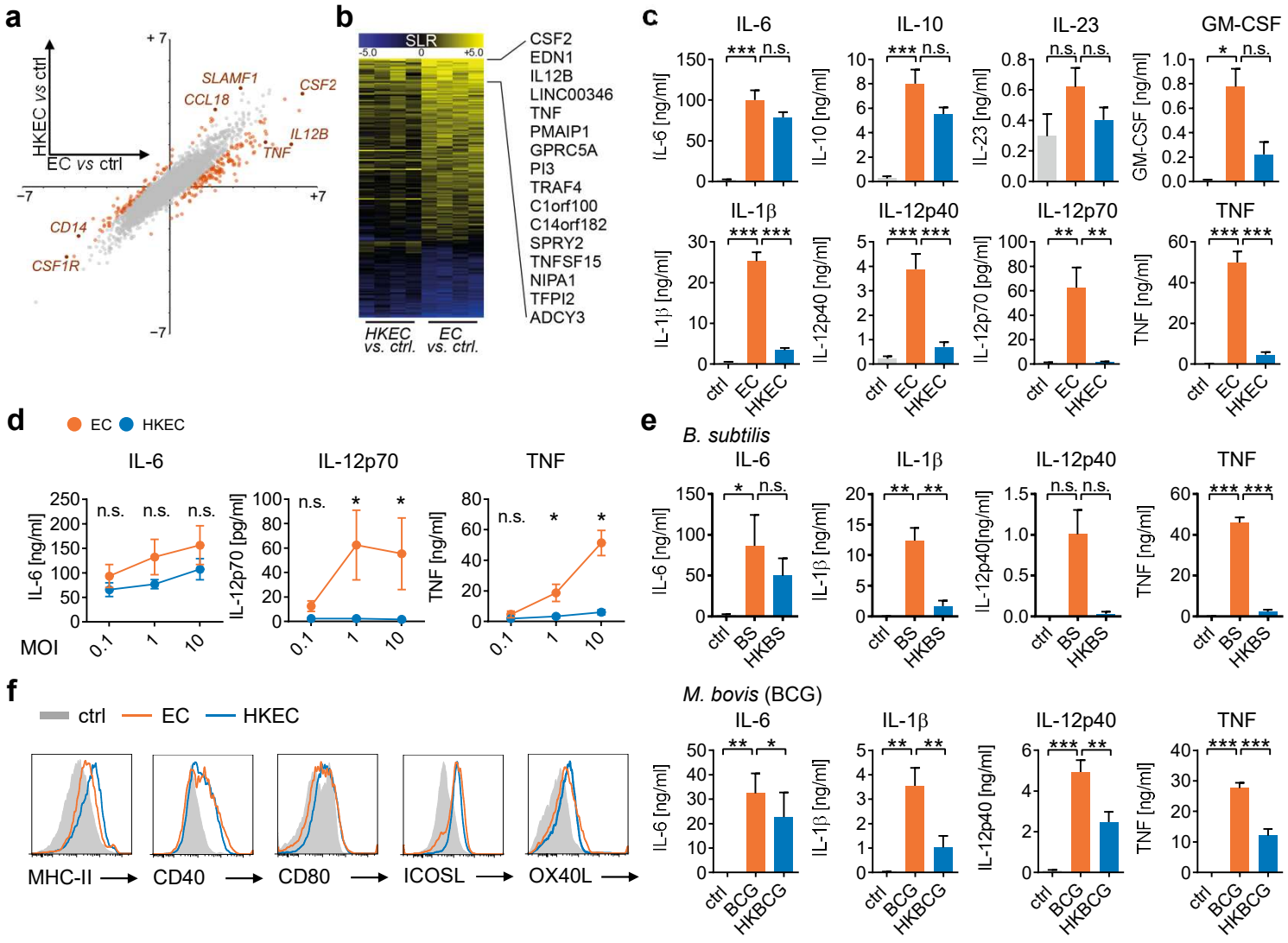
a
HKEC vs ctrl
EC vs ctrl
SLAMF1
CCL18
CSF2
IL12B
TNF
CD14
CSF1R
b
SLR
CSF2
EDN1
IL12B
LINC00346
TNF
PMAIP1
GPRC5A
PI3
TRAF4
C1orf100
C14orf182
SPRY2
TNFSF15
NIPA1
TFPI2
ADCY3
HKEC vs. ctrl.
EC vs. ctrl.
c
IL-6
IL-10
IL-23
GM-CSF
IL-1β
IL-12p40
IL-12p70
TNF
ctrl
EC
HKEC
d
EC
HKEC
IL-6
IL-12p70
TNF
MOI
e
B. subtilis
BS
HKBS
M. bovis (BCG)
BCG
HKBCG
f
ctrl
EC
HKEC
MHC-II
CD40
CD80
ICOSL
OX40L

Fig. 4

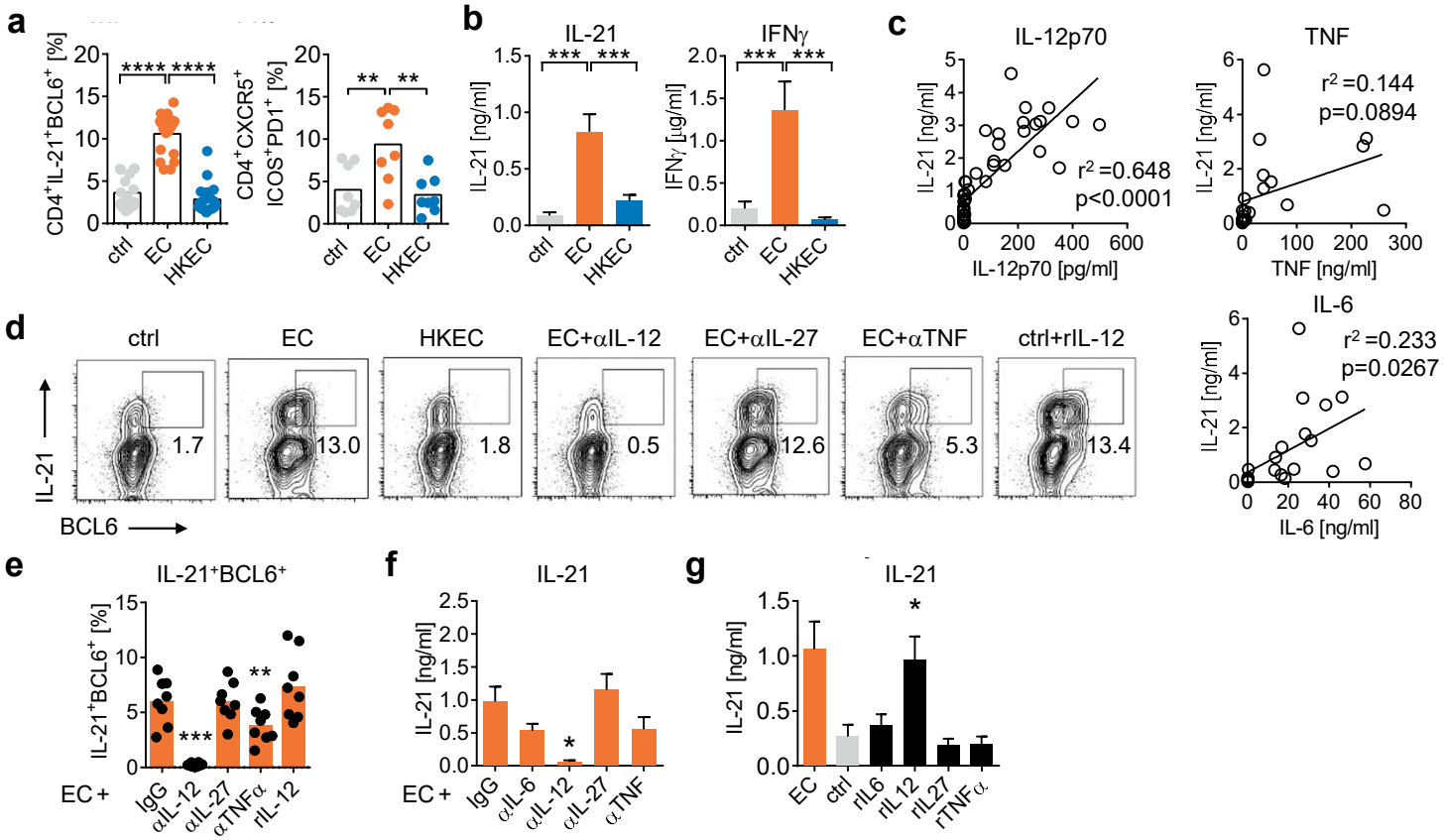
a
CD4+IL-21+BCL6+ [%]
CD4+CXCR5+ ICOS+PD1+ [%]
ctrl
EC
HKEC
b
IL-21
IFNγ
IL-21 [ng/ml]
IFNγ [μg/ml]
c
IL-12p70
IL-21 [ng/ml]
IL-12p70 [pg/ml]
r2 =0.648
p<0.0001
TNF
TNF [ng/ml]
r2 =0.144
p=0.0894
IL-6
IL-6 [ng/ml]
r2 =0.233
p=0.0267
d
ctrl
EC
HKEC
EC+αIL-12
EC+αIL-27
EC+αTNF
ctrl+rIL-12
IL-21
BCL6
1.7
13.0
1.8
0.5
12.6
5.3
13.4
e
IL-21+BCL6+
IL-21+BCL6+ [%]
EC +
IgG
αIL-12
αIL-27
αTNFα
rIL-12
f
IL-21
IL-21 [ng/ml]
EC +
IgG
αIL-6
αIL-12
αIL-27
αTNF
g
IL-21
IL-21 [ng/ml]
EC
ctrl
rIL6
rIL12
rIL27
rTNFα

Fig. 5

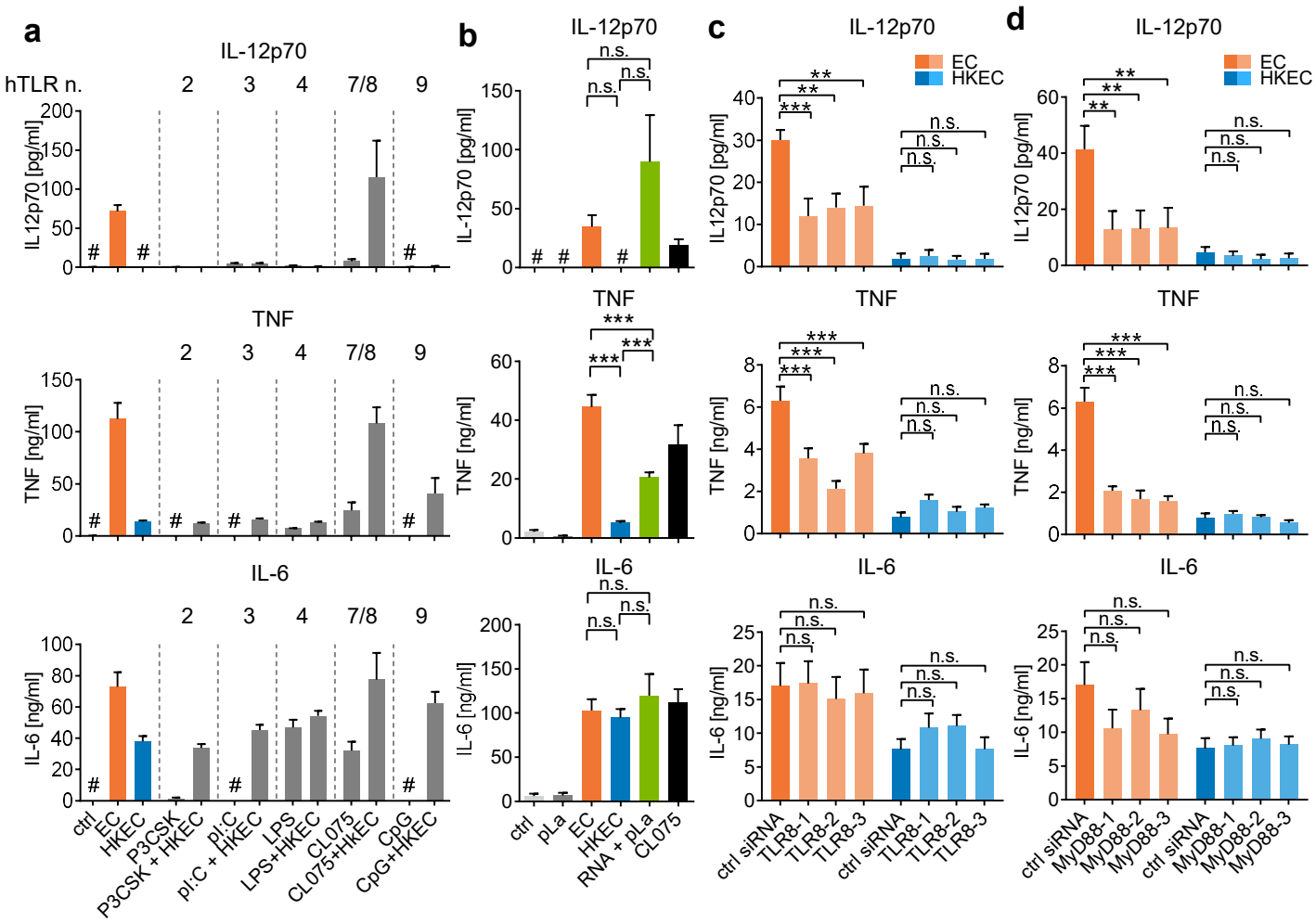
a
IL-12p70
hTLR n.
2
3
4
7/8
9
IL 12p70 [pg/ml]
TNF
TNF [ng/ml]
IL-6
IL-6 [ng/ml]
ctrl
EC
HKEC
P3CSK
P3CSK + HKEC
pI:C
pI:C + HKEC
LPS
LPS+HKEC
CL075
CL075+HKEC
CpG
CpG+HKEC
b
IL-12p70
IL-12p70 [pg/ml]
TNF
TNF [ng/ml]
IL-6
IL-6 [ng/ml]
ctrl
pLa
EC
HKEC
RNA + pLa
CL075
c
IL-12p70
EC
HKEC
IL12p70 [pg/ml]
TNF
TNF [ng/ml]
IL-6
IL-6 [ng/ml]
ctrl siRNA
TLR8-1
TLR8-2
TLR8-3
d
IL-12p70
EC
HKEC
IL12p70 [pg/ml]
TNF
TNF [ng/ml]
IL-6
IL-6 [ng/ml]
ctrl siRNA
MyD88-1
MyD88-2
MyD88-3
n.s.
**
***

Fig. 6

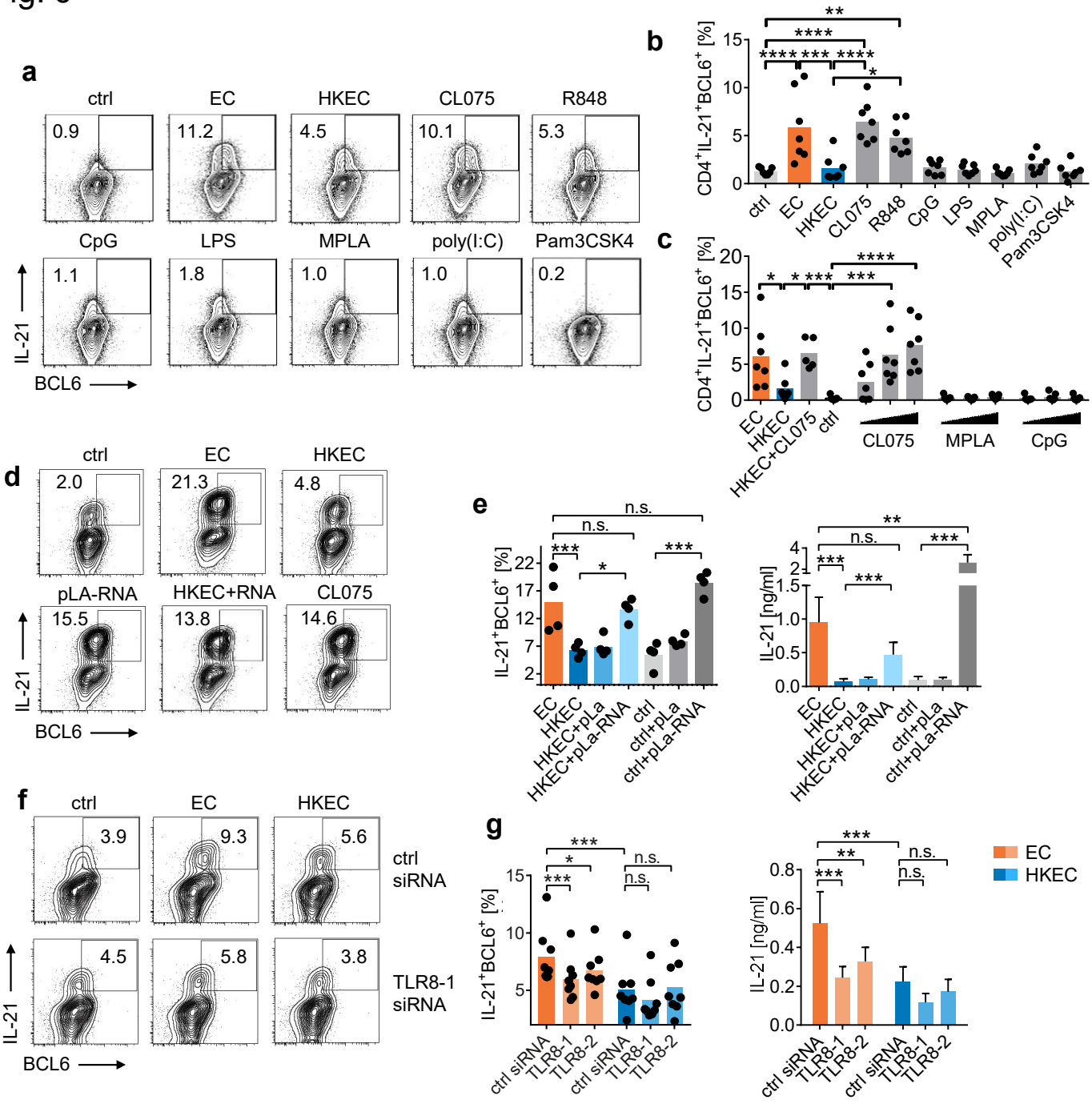
a
ctrl
EC
HKEC
CL075
R848
0.9
11.2
4.5
10.1
5.3
CpG
LPS
MPLA
poly(I:C)
Pam3CSK4
1.1
1.8
1.0
1.0
0.2
IL-21
BCL6
b
CD4+IL-21+BCL6+ [%]
ctrl
EC
HKEC
CL075
R848
CpG
LPS
MPLA
poly(I:C)
Pam3CSK4
c
CD4+IL-21+BCL6+ [%]
EC
HKEC
HKEC+CL075
ctrl
CL075
MPLA
CpG
d
ctrl
EC
HKEC
2.0
21.3
4.8
pLA-RNA
HKEC+RNA
CL075
15.5
13.8
14.6
IL-21
BCL6
e
IL-21+BCL6+ [%]
IL-21 [ng/ml]
EC
HKEC
HKEC+pLa
HKEC+pLa-RNA
ctrl
ctrl+pLa
ctrl+pLa-RNA
f
ctrl
EC
HKEC
3.9
9.3
5.6
ctrl siRNA
4.5
5.8
3.8
TLR8-1 siRNA
IL-21
BCL6
g
IL-21+BCL6+ [%]
IL-21 [ng/ml]
ctrl siRNA
TLR8-1
TLR8-2
EC
HKEC

Fig. 7

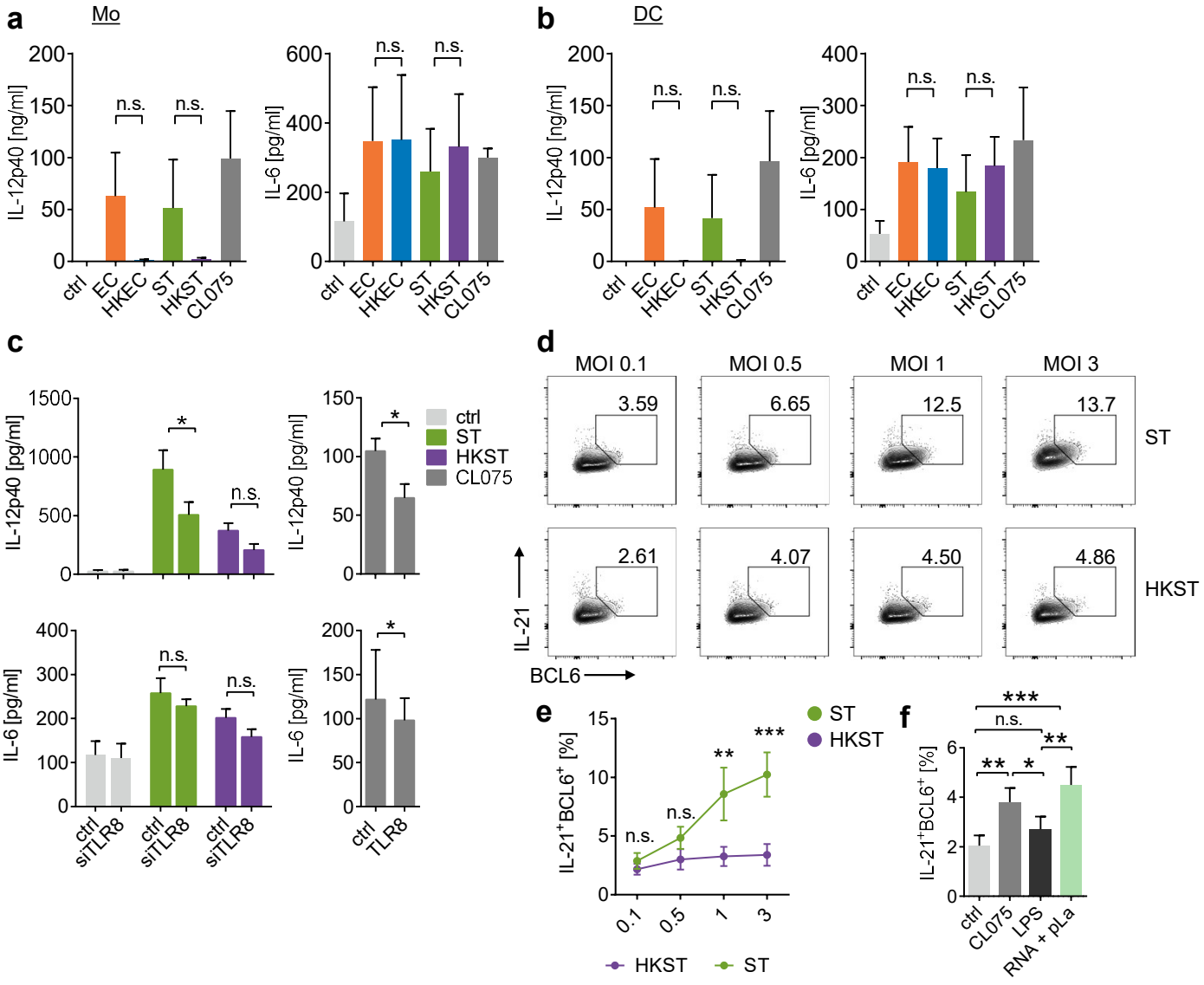
a
Mo
IL-12p40 [ng/ml]
IL-6 [pg/ml]
n.s.
ctrl
EC
HKEC
ST
HKST
CL075
b
DC
c
IL-12p40 [pg/ml]
IL-6 [pg/ml]
*
ctrl
ST
HKST
CL075
siTLR8
TLR8
d
MOI 0.1
MOI 0.5
MOI 1
MOI 3
3.59
6.65
12.5
13.7
2.61
4.07
4.50
4.86
IL-21
BCL6
e
IL-21+BCL6+ [%]
**
***
f
LPS
RNA + pLa

Fig. 8

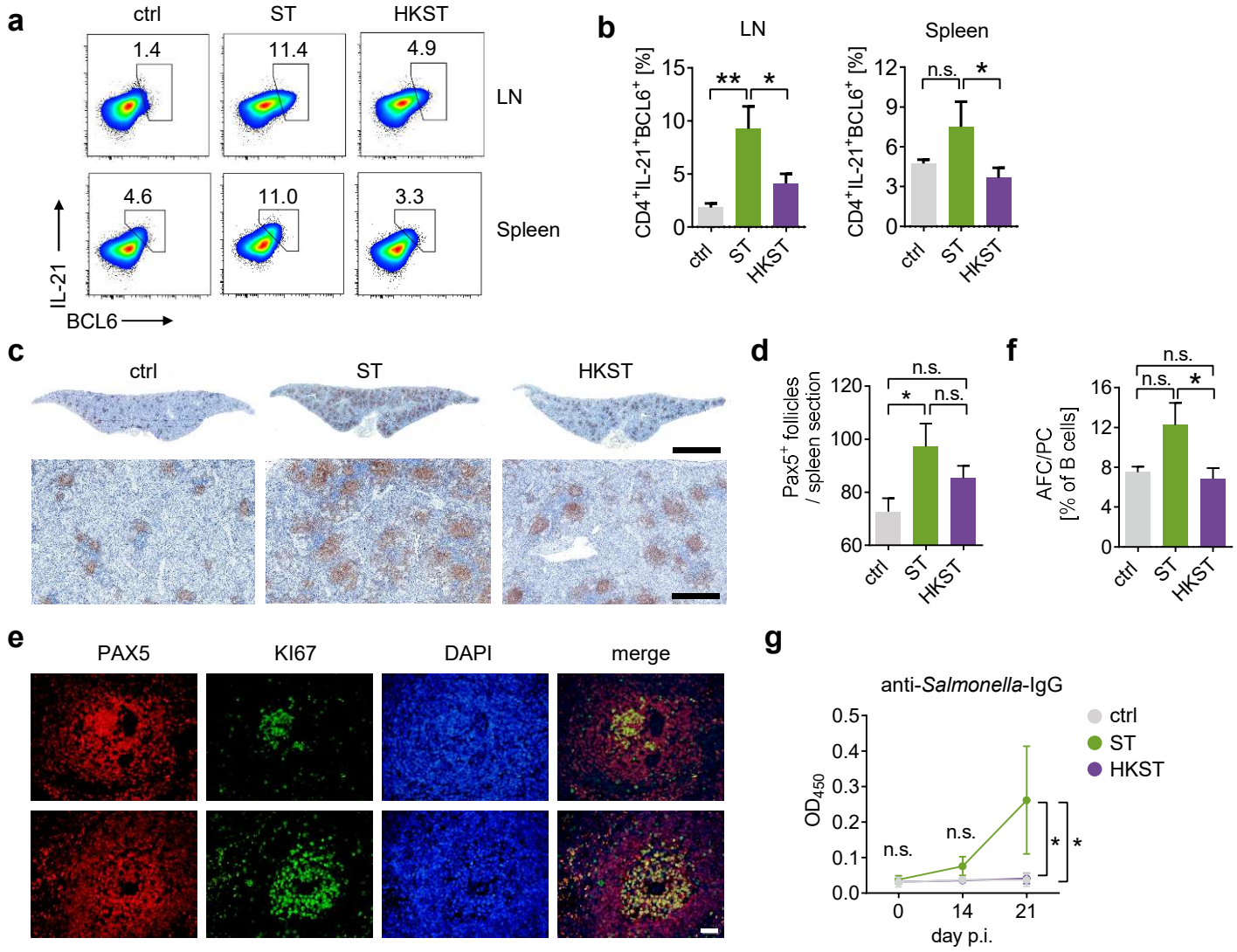
a
ctrl
ST
HKST
1.4
11.4
4.9
LN
4.6
11.0
3.3
Spleen
IL-21
BCL6
b
LN
Spleen
CD4+IL-21+BCL6+ [%]
**
*
n.s.
*
ctrl
ST
HKST
c
ctrl
ST
HKST
d
Pax5+ follicles / spleen section
n.s.
*
n.s.
f
AFC/PC [% of B cells]
n.s.
n.s.
*
e
PAX5
KI67
DAPI
merge
g
anti-Salmonella-IgG
OD450
ctrl
ST
HKST
n.s.
n.s.
*
*
0
14
21
day p.i.

Fig. 9

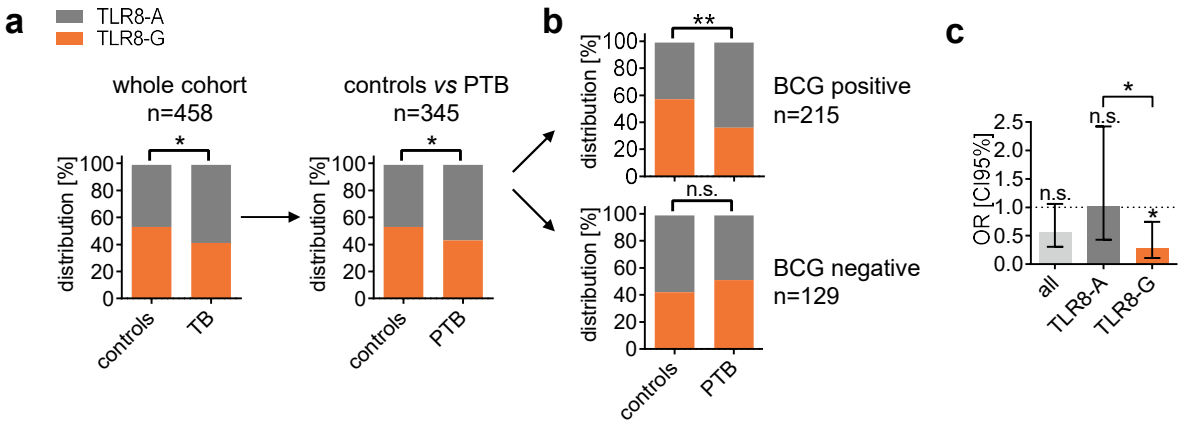
a
TLR8-A
TLR8-G
whole cohort
n=458
distribution [%]
controls
TB
controls vs PTB
n=345
controls
PTB
b
BCG positive
n=215
BCG negative
n=129
n.s.
c
OR [CI95%]
n.s.
all
TLR8-A
TLR8-G